



HAL
open science

Inflammasome Regulates Hematopoiesis through Cleavage of the Master Erythroid Transcription Factor GATA1

Sylwia D Tyrkalska, Ana B Pérez-Oliva, Lola Rodríguez-Ruiz, Francisco J Martínez-Morcillo, Francisca Alcaraz-Pérez, Francisco J Martínez-Navarro, Christophe Lachaud, Nouraz Ahmed, Timm Schroeder, Irene Pardo-Sánchez, et al.

► **To cite this version:**

Sylwia D Tyrkalska, Ana B Pérez-Oliva, Lola Rodríguez-Ruiz, Francisco J Martínez-Morcillo, Francisca Alcaraz-Pérez, et al.. Inflammasome Regulates Hematopoiesis through Cleavage of the Master Erythroid Transcription Factor GATA1. *Immunity*, 2019, Epub ahead of print. 10.1016/j.immuni.2019.05.005 . hal-02148333

HAL Id: hal-02148333

<https://hal.science/hal-02148333>

Submitted on 5 Jun 2019

HAL is a multi-disciplinary open access archive for the deposit and dissemination of scientific research documents, whether they are published or not. The documents may come from teaching and research institutions in France or abroad, or from public or private research centers.

L'archive ouverte pluridisciplinaire **HAL**, est destinée au dépôt et à la diffusion de documents scientifiques de niveau recherche, publiés ou non, émanant des établissements d'enseignement et de recherche français ou étrangers, des laboratoires publics ou privés.

1 **INFLAMMASOME REGULATES HEMATOPOIESIS THROUGH CLEAVAGE**
2 **OF THE MASTER ERYTHROID TRANSCRIPTION FACTOR GATA1**

3
4 Sylwia D. Tyrkalska^{1,&#}, Ana B. Pérez-Oliva^{1,#,*}, Lola Rodríguez-Ruiz¹, Francisco J.
5 Martínez-Morcillo¹, Francisca Alcaraz-Pérez², Francisco J. Martínez-Navarro¹,
6 Christophe Lachaud³, Nouraz Ahmed⁴, Timm Schroeder⁴, Irene Pardo-Sánchez¹,
7 Sergio Candel^{1,§}, Azucena López-Muñoz¹, Avik Choudhuri⁵, Marlies P. Rossmann⁵,
8 Leonard I. Zon^{5,6}, María L. Cayuela², Diana García-Moreno^{1,*}, Victoriano Mulero^{1,*},[¶]

9 ¹Universidad de Murcia, IMIB-Arrixaca, Murcia, Spain.

10 ²Hospital Clínico Universitario Virgen de la Arrixaca, IMIB-Arrixaca, Murcia, Spain.

11 ³Aix-Marseille University, Inserm, CNRS, Institut Paoli-Calmettes, CRCM, Marseille,
12 France.

13 ⁴Department of Biosystems Science and Engineering, ETH Zurich, Basel, Switzerland.

14 ⁵Harvard University, Cambridge, MA 02138, USA; Stem Cell Program and Division of
15 Hematology/Oncology, Children's Hospital Boston, Howard Hughes Medical Institute,
16 Boston, MA 02115, USA.

17 ⁶Dana-Farber Cancer Institute, Boston, MA 02215, USA; Harvard Stem Cell Institute,
18 Boston, MA 02115, USA; Harvard Medical School, Boston, MA 02115, USA.

19
20 [&]Current address: Cambridge Institute for Medical Research, University of Cambridge,
21 Cambridge CB2 0XY, UK.

22 [§]Current address: Department of Medicine, University of Cambridge, MRC Laboratory
23 of Molecular Biology, Cambridge CB2 0QH, UK.

24 [#]These authors contributed equally

25
26 ^{*}Corresponding authors: ABPO (anabpo@um.es), DGM (dianagm@um.es) and VM
27 (vmulero@um.es)

28 [¶]Lead contact: VM (vmulero@um.es)

30 **Summary (word count 149)**

31

32 Chronic inflammatory diseases are associated with altered hematopoiesis that
33 could result in neutrophilia and anemia. Here we report that genetic or chemical
34 manipulation of different inflammasome components altered the differentiation of
35 hematopoietic stem and progenitor cells (HSPC) in zebrafish. Although the
36 inflammasome was dispensable for the emergence of HSPC, it was intrinsically
37 required for their myeloid differentiation. In addition, Gata1 transcript and protein
38 amounts increased in inflammasome-deficient larvae, enforcing erythropoiesis and
39 inhibiting myelopoiesis. This mechanism is evolutionarily conserved, since
40 pharmacological inhibition of the inflammasome altered erythroid differentiation of
41 human erythroleukemic K562 cells. In addition, caspase-1 inhibition rapidly
42 upregulated GATA1 protein in mouse HSPC promoting their erythroid differentiation.
43 Importantly, pharmacological inhibition of the inflammasome rescued zebrafish disease
44 models of neutrophilic inflammation and anemia. These results indicate that the
45 inflammasome plays a major role in the pathogenesis of neutrophilia and anemia of
46 chronic diseases and reveal druggable targets for therapeutic interventions.

47

48 **Keywords:** Hematopoiesis, GATA1, Caspase-1, inflammasome, anemia, neutrophilic
49 inflammation, zebrafish, mouse.

50

51

52 **Introduction**

53 Hematopoiesis is the process of blood cell formation that occurs during
54 embryonic development and across adulthood to produce the blood system
55 (Jagannathan-Bogdan and Zon, 2013). In vertebrates, blood development involves two
56 main waves of hematopoiesis: the primitive one during early embryonic development,
57 and the definitive one, which occurs in later stages (Gore et al., 2018). Definitive
58 hematopoiesis engages multipotent hematopoietic stem cells (HSC), which migrate
59 eventually to the bone marrow, or kidney marrow in zebrafish, and give rise to all blood
60 lineages (Birbrair and Frenette, 2016; Cumano and Godin, 2007). HSC maturation
61 involves the diversification of the lymphoid (T, B and NK cells) and myeloid and
62 erythroid cell lineages (megakaryocytes, erythrocytes, granulocytes and macrophages)
63 (Kondo, 2010; Kondo et al., 2003; Weissman, 2000). The decision for erythroid and
64 myeloid fates depends mainly on two transcription factors GATA1 and SPI1 (also
65 known as PU.1) that show a cross-inhibitory relationship resulting in physical
66 interaction and direct competition between them for target genes (Nerlov et al., 2000;
67 Rekhtman et al., 1999). However, there are many controversies about the factors
68 responsible for terminal erythroid and myeloid differentiation and many unknown
69 pathways being probably involved in its regulation (Cantor and Orkin, 2002; Hoppe et
70 al., 2016). These unidentified pathways might have important clinical implications,
71 since hematopoietic lineage bias is associated with increased incidence of diseases with
72 prominent inflammatory components including atherosclerosis, autoimmunity,
73 neurodegenerative disease, and carcinogenesis (Elias et al., 2017).

74 The inflammasomes are part of innate immune system and as intracellular
75 receptors and sensors, they regulate the activation of inflammatory caspases, namely
76 caspase-1 and caspase-11, which induce inflammation in response to infectious
77 microbes and endogenous danger signals (Latz et al., 2013; Martinon et al., 2009).
78 Typically inflammasome multiprotein complexes contain sensor proteins (nucleotide
79 binding domain and leucine rich repeat gene family, NLRs), adaptor proteins
80 (Apoptosis-associated speck-like protein containing a CARD, ASC), and effector
81 caspases in a zymogen form, all being able to interact among themselves by homotypic
82 interactions (Broz and Monack, 2011; Sharma and Kanneganti, 2016). Recently, it has
83 been shown that also guanylate binding protein (GBP) protein family forms part of
84 these multiprotein complexes (Pilla et al., 2014; Santos et al., 2018; Tyrkalska et al.,
85 2016; Wallet et al., 2017; Zwack et al., 2017). Oligomerization of pro-caspases and

86 their autoproteolytic maturation lead to the processing and secretion of the pro-
87 inflammatory cytokines interleukin-1 β (IL-1 β) and IL-18, and the induction of a form of
88 programmed cell death called pyroptosis (Lamkanfi and Dixit, 2014). Lately, it has been
89 reported that inflammasomes play crucial roles not only in infection and sterile
90 inflammation but also in maintaining the basic cellular functions and controlling cellular
91 homeostasis (Rathinam and Fitzgerald, 2016). Hence, additional uncovered regulatory
92 functions for the inflammasomes have been shown in cell metabolism, proliferation,
93 gene transcription and tumorigenesis (Rathinam and Fitzgerald, 2016; Sharma and
94 Kanneganti, 2016). Although up to date little is known about the impact of the
95 inflammasomes on hematopoiesis in general, it has been shown that the master
96 erythroid transcription factor GATA1 can be cleaved *in vitro* by many caspases and *in*
97 *vivo* by caspase-3 (De Maria et al., 1999).

98 Zebrafish has recently arisen as a powerful and useful model to study
99 hematopoiesis (Berman et al., 2012; Ellett and Lieschke, 2010). Moreover, the genetic
100 programs controlling hematopoiesis in the zebrafish are conserved with mammals,
101 including humans, making them clinically relevant model systems (Jagannathan-
102 Bogdan and Zon, 2013). Here we show the critical role played by the inflammasome in
103 the regulation of erythroid and myeloid cell fate decision, and terminal erythroid
104 differentiation. Furthermore, the results also have important clinical implications, since
105 pharmacological inhibition of the inflammasome rescued zebrafish disease models of
106 neutrophilic inflammation and anemia.

107

108 **Results**

109

110 *Inflammasome inhibition decreases the number of neutrophils and macrophages in*
111 *zebrafish larvae*

112 Using zebrafish transgenic lines with green fluorescent neutrophils
113 *Tg(mpx:eGFP)ⁱ¹¹⁴* or macrophages *Tg(mpeg1:eGFP)^{g122}*, we quantitated the total
114 number of both cell populations in whole larvae at 72 hpf. Genetic inhibition of several
115 inflammasome components, namely Gbp4 and Asc resulted in significant decreased
116 numbers of both neutrophils (Figure 1A, 1B) and macrophages (Figure S1A, S1B).
117 Similarly, pharmacological inhibition of caspase-1 with the irreversible inhibitor Ac-
118 YVAD-CMK (Tyrkalska et al., 2016) also resulted in decreased numbers of myeloid

119 cells (Figure 1C, 1D, S1C, S1D). These results were confirmed using an independent
120 transgenic line *Tg(lyz:dsRED)^{nz50}* with labeled neutrophils (Figure S2A-S2D).
121 Similarly, forced expression of the GTPase-deficient mutant of Gbp4 (KS/AA) as well
122 as its double mutant (DM: KS/AA; Δ CARD), both of which behave as dominant
123 negatives (DN) and inhibit inflammasome-dependent caspase-1 activation (Tyrkalska et
124 al., 2016), resulted in decreased neutrophil number (Figure 1E, 1F). In addition,
125 although activation of the inflammasome by forced expression of either Gbp4 or Asc
126 failed to increase neutrophil (Figure 1E-1H) or macrophage (Figure S1E-S1F) numbers,
127 it was able to rescue myeloid cell number and caspase-1 activity Asc-deficient fish
128 (Figure 1G, 1H). Notably, however, simultaneous expression of Asc and Caspa, the
129 functional homolog of mammalian CASP1 (Kuri et al., 2017; Masumoto et al., 2003;
130 Tyrkalska et al., 2016), significantly increased the number of neutrophils (Figure 1I, 1J)
131 and macrophages (Figure S1E, S1F).

132

133 *The inflammasome regulates HSPC differentiation but is dispensable for their*
134 *emergence*

135 The differentiation of hematopoietic stem and progenitor cells (HSPC) into
136 various blood cell types is controlled by multiple extrinsic and intrinsic factors and the
137 deregulation in hematopoiesis can result in a number of hematological abnormalities
138 (Morrison et al., 1997; Yang et al., 2007). Chronic inflammatory disorders are usually
139 associated to neutrophilia and anemia, the so-called anemia of chronic diseases (ACD).
140 Therefore, we next examined if the inflammasome also regulated erythropoiesis using a
141 zebrafish transgenic line *Tg(lcr:eGFP)*, which has specific erythroid GFP expression
142 (Ganis et al., 2012). The results showed that inflammasome activity had the inverse
143 effect on erythrocytes than on myeloid cells; that is, erythrocyte abundance increased
144 following genetic and pharmacological inflammasome inhibition, as assayed by flow
145 cytometry (Figures 1K, 1L and S3). However, the expression of *cmyb* and *runx1*, which
146 begins by 36 hpf and marks emerging definitive HSPC (Burns et al., 2005), was
147 unaffected in guanylate binding protein-4 (Gbp4)- and Asc-deficient larvae at 48 hpf, as
148 assayed by whole-mount in situ hybridization (WISH) (Figure S4). Similarly, the
149 expression of *rag1*, which is expressed in differentiated thymic T cells was apparently
150 unaffected by 5 dpf in inflammasome-deficient larvae (Figure S4). Collectively, these

151 results suggest a specific role of the inflammasome in the regulation of the balance
152 between myelopoiesis and erythropoiesis.

153 To further confirm the role of the inflammasome in HSPC differentiation, we
154 quantitated the number of HSPC in the transgenic line *Tg(runx1:GAL4; UAS:nfsB-*
155 *mCherry)* which has fluorescently labeled HSPC (Tamplin et al., 2015), upon genetic or
156 pharmacological inhibition of the inflammasome at different developmental stages (24
157 and 48 hpf). Inhibition of caspase-1 resulted in no changes in HSPC number at any
158 point of the treatment, the result being confirmed in *Asc*-deficient larvae (Figure 2A-H).
159 Furthermore, genetic inhibition of the inflammasome in neutrophils and HSPC by
160 forced expression of DN forms of *Asc* (*Asc*ΔCARD) or *Gbp4* (*Gbp4KS/AA*)
161 (Tyrkalska et al., 2016) using the specific promoters *mpx* and *runx1*, respectively,
162 showed that the number of neutrophils declined in HSPC, but not in neutrophil,
163 inflammasome-deficient larvae (Figure 2I-2L). Collectively these results confirm the
164 dispensability of the inflammasome for HSPC emergence and renewal, but that is
165 intrinsically required for HSPC differentiation.

166 Zebrafish is an elegant model for cell ablation by use of the specific transgenic
167 lines that expresses the bacterial nitroreductase, encoded by the *nfsB* gene, under the
168 control of specific promoters (Davison et al., 2007). The nitroreductase enzyme
169 converts the drug metronidazole (Mtz) to a cytotoxic product, which induces cell death
170 in expressing cells to achieve tissue-specific ablation having no effect on other cell
171 populations (Curado et al., 2007; Curado et al., 2008; Prajsnar et al., 2012). Using this
172 approach, we ablated neutrophils in *Tg(mpx:Gal4; UAS:nfsB-mCherry)* zebrafish by
173 applying Mtz for 24h and then analyzed neutrophil recovery in the presence or absence
174 of the caspase-1 inhibitor for 6 days (Figure 3). Mtz robustly reduced neutrophil
175 number, which began to recover by 4 days post-ablation in control larvae (Figure 3).
176 However, pharmacological inhibition of the inflammasome impaired neutrophil
177 recovery upon ablation and strongly decreased neutrophil abundance in non-ablated
178 larvae (Figure 3). As expected, continuous Mtz treatment resulted in drastic neutrophil
179 decline but did not show any toxic effect on control larvae that did not express the
180 nitroreductase (Figure 3). These results indicate that the inflammasome is indispensable
181 for myeloid differentiation of HSPC.

182

183

184 *Inflammasome inhibition impairs demand-driven myelopoiesis*

185 In response to infection, the hematopoietic tissue enhances production and
186 mobilization of neutrophils, which have short lifespan and are needed in large numbers
187 to fight infections. This process is called demand-driven or emergency hematopoiesis
188 (Hall et al., 2012). To check whether only steady-state or also demand-driven
189 hematopoiesis were regulated by the inflammasome, we infected with *Salmonella*
190 *enterica* serovar Typhimurium in the otic vesicle of 48 hpf larvae and counted total
191 neutrophil numbers at 24 hpi in the presence or absence of the irreversible caspase-1
192 inhibitor Ac-YVAD-CMK. It was observed that pharmacological inhibition of the
193 inflammasome was able to abrogate infection-driven myelopoiesis, which resulted in
194 increased number of neutrophils in infected larvae (Figure 4A, 4B). Notably, forced
195 expression of granulocyte colony-stimulating factor (Gcsf), which stimulates both
196 steady-state and demand-driven granulopoiesis in zebrafish (Hall et al., 2012; Stachura
197 et al., 2013), increased neutrophil number to similar amounts in wild type and Asc-
198 deficient larvae, as well as in larvae treated with the caspase-1 inhibitor, without
199 affecting caspase-1 activity (Figure 4C-4F). Nevertheless, Gcsf was unable to rescue the
200 higher susceptibility to *S. Typhimurium* infection of Asc-deficient and caspase-1
201 inhibitor-treated larvae (Figure 4G, 4H), confirming previous results in Gbp4-deficient
202 larvae (Tyrkalska et al., 2016). All these results also suggest that the inflammasome
203 regulates the myeloid and erythroid fate decision besides the function of mature
204 myeloid cells.

205

206 *The inflammasome shifts the spi1/gata1 balance favoring myeloid differentiation*

207 The regulation of Spi1 and Gata1 has been shown to be critical for the
208 differentiation of myeloid and erythroid cells, respectively, in all vertebrates. As
209 inhibition of the inflammasome resulted in a hematopoietic lineage bias, that is, reduced
210 myeloid and increased erythroid blood cells, we next analyzed *spi1* and *gata1* transcript
211 amounts by RT-qPCR and whole-mount *in situ* hybridization (WISH). We observed
212 decreased *spi1/gata1* transcript ratio at 24 hpf in Gbp4- and Asc-deficient larvae, while
213 the transcript amounts of the genes encoding Spi1-downstream pivotal macrophage and
214 neutrophil growth factors, namely macrophage- and granulocyte colony stimulating
215 factors (*mcsf* and *gcsf* genes), were unaffected (*mcsf* and *gcsf*) (Figures 4I, S4).
216 Importantly, Gata1 protein amounts were also fine-tuned by the inflammasome, since

217 genetic inhibition of either Asc or Gbp4 was able to increase Gata1, while forced
218 expression of Asc and Caspa, which resulted in increased number of neutrophils and
219 macrophages (Figure 1I, 1J, S1E, S1F), robustly decreased Gata1 (Figure 4J).
220 Therefore, the inflammasome regulates HSPC fate decision through fine-tuning Gata1
221 amounts.

222

223 *The regulation of HSPC differentiation by the inflammasome is evolutionarily*
224 *conserved*

225 We next sought to determine if the inflammasome also regulates mouse
226 hematopoiesis. We quantified the impact of CASP1 inhibition on GATA1 and SPI1
227 protein amounts in single mouse hematopoietic stem cells (HSC) using time-lapse
228 microscopy immediately following their isolation. Time-lapse movies were acquired for
229 24 h to quantify early dynamics in GATA1 amounts before the first cell division using a
230 homozygous and extensively validated GATA1 and SPI1 reporter mouse line
231 expressing a fusion of GATA1 and monomeric Cherry (mCherry) and SPI1 and
232 enhanced yellow fluorescent protein (eYFP) from the endogenous *Gata1* and *Spil*
233 genomic loci, respectively (Hoppe et al., 2016). Inhibition of CASP1 up-regulated
234 Gata1-mCherry protein in differentiating HSC within 18 h, while SPI1-eYFP protein
235 amounts were unaffected (Figures 5A-5C). In line with these results, CASP1 inhibition
236 increased megakaryocyte-erythrocyte (MegE) colony output of mouse HSCs at expense
237 of granulocyte-monocyte (GM) colonies (Figure 5D). These data demonstrate that at the
238 time of normal lineage decision making in HSC, the manipulation of GATA1 protein
239 amounts through the inflammasome can alter lineage choice, further confirming our *in*
240 *vivo* studies in zebrafish.

241 To further explore the relevance of the inflammasome in erythroid
242 differentiation, we then used the human erythroleukemic K562 cell line, which can be
243 differentiated to erythrocytes in the presence of hemin (Andersson et al., 1979; Koeffler
244 and Golde, 1980). GATA1 amounts and activity were found to increase in the early
245 stages of erythropoiesis, while they decreased in the late phase to allow terminal
246 erythroid differentiation (Ferreira et al., 2005; Whyatt et al., 2000). As expected, we
247 observed that hemin promoted gradual hemoglobin accumulation and decreased
248 GATA1 protein amounts from 0 to 48 h (Figure 6A, 6D). Notably, the transcript

249 amounts of *NLRC4*, *NLRP3* and *CASP1* gradually increased, while those of *PYCARD*
250 peaked at 12 h and then declined to basal amounts (Figure S5). Furthermore, *CASP1*
251 activity (Figure 6B) and protein amounts (Figure 6C) progressively increased during
252 erythroid differentiation, and *CASP1* was uniformly distributed in both the cytosol and
253 the nucleus (Figure 6C). In addition, pharmacological inhibition of *CASP1* in K562
254 cells impaired hemin-induced erythroid differentiation, assessed as hemoglobin
255 accumulation, and inhibited GATA1 decline at both 24 (Figure 6E) and 48 h (Figure 6F,
256 6G). As the Ac-YVAD-CMK inhibitor may also inhibit *CASP4*, we used the *CASP4*
257 and *CASP5* inhibitor Ac-LEVD-CHO and found that it failed to affect the erythroid
258 differentiation of K562 cells and their GATA1 amounts (Figure S6A).

259 *CASP1* may target several proteins to regulate HSPC differentiation. One
260 possibility is that *CASP1* directly cleaves GATA1, as it has been reported for *CASP3*,
261 which negatively regulates erythropoiesis through GATA1 cleavage (De Maria et al.,
262 1999). Therefore, we studied whether recombinant human *CASP1* was able to cleave
263 human GATA1 *in vitro*. The results showed that recombinant *CASP1* cleaved GATA1
264 generating N- and C-terminal proteolytic fragments of about 30 and 15 kDa,
265 respectively (Figure S7A-S7C). *CASP1* cleavage of GATA1 at residues D276 and/or
266 D300 may generate the obtained fragments, so we generated single and double *CASP1*
267 mutants (D276E and D300E) and found that *CASP1* was only able to cleave GATA1 at
268 residue D300 (Figure S7D). Collectively, all these results uncover an evolutionarily
269 conserved role of the inflammasome in the regulation of erythroid vs. myeloid fate
270 decision and terminal erythroid differentiation via cleavage of GATA1.

271

272 *Pharmacological inhibition of the inflammasome rescues zebrafish models of* 273 *neutrophilic inflammation and anemia*

274 Hematopoietic lineage bias is associated with chronic inflammatory diseases,
275 cancer and aging (Elias et al., 2017; Marzano et al., 2018; Wu et al., 2014). Neutrophilic
276 dermatosis are a group of diseases characterized by the accumulation of neutrophils in
277 the skin (Marzano et al., 2018). We used a zebrafish *Spint1a*-deficient line as model of
278 neutrophilic dermatosis, since it is characterized by strong neutrophil infiltration into
279 the skin (Carney et al., 2007; Mathias et al., 2007). It was found that *Spint1a*-deficient
280 larvae had increased caspase-1 activity (Figure 7A) and an altered *spil/gata1* ratio
281 (Figure 7B). Notably, although pharmacological inhibition of caspase-1 failed to rescue

282 neutrophil skin infiltration of *Spint1a*-deficient animals (Figure 7C, 7E), it was able to
283 rescue their robust neutrophilia (Figure 7D, 7E). Similarly, genetic inactivation of *caspa*
284 with CRISPR-Cas9 also rescued neutrophilia, but not neutrophil infiltration, of *Spint1a*-
285 deficient animals (Figure 7F, 7G). However, CASP4 and CASP5 inhibition failed to
286 rescue both neutrophilia and neutrophil infiltration in this animal model (Figure S6B).

287 We next model Diamond-Blackfan anemia, a ribosomopathy caused by
288 inefficient translation of GATA1 (Danilova and Gazda, 2015), in zebrafish larvae by
289 reducing *Gata1* amounts using a specific morpholino. We firstly titrated the morpholino
290 and found that 1.7 ng/egg resulted in larvae with mild, moderate and severe anemia
291 (Figure 7H), while 0.85 ng/egg and 3.4 ng/egg had little or drastic effects, respectively
292 (data not shown). We thus examined whether pharmacological inhibition of caspase-1
293 could rescue hemoglobin alterations of *Gata1*-deficient larvae. For these experiments,
294 we treated larvae with the reversible inhibitor of caspase-1 Ac-YVAD-CHO for 24 to
295 48 hpf and analyzed hemoglobin at 72 hpf to allow terminal erythroid differentiation in
296 the absence of caspase-1 inhibition. The results show that treatment of larvae for 24 h
297 with this reversible inhibitor of caspase-1 partially rescued hemoglobin defects in
298 *Gata1*-deficient larvae and *Spi1/Gata1* protein ratio (Figure 7I, 7J). These results taken
299 together demonstrate that pharmacological inhibition of caspase-1 rescues
300 hematopoietic lineage bias *in vivo*.

301

302 **Discussion**

303 We report here an evolutionarily conserved signaling pathway which links the
304 inflammasome with HSPC differentiation. Although previous reports have shown that
305 proinflammatory signals are indispensable for HSPC emergence (Espin-Palazon et al.,
306 2018), the roles of these signals, and in particular the inflammasome, in HSPC
307 formation, maintenance and differentiation are largely unknown. During periods of
308 hematopoietic stress induced by chemotherapy or viral infection, activation of NLRP1a
309 prolongs cytopenia, bone marrow hypoplasia, and immunosuppression (Masters et al.,
310 2012). This effect is mediated by the CASP1-dependent, but ASC-independent,
311 pyroptosis of hematopoietic progenitor cells (Masters et al., 2012). In addition, the
312 NLRP3 inflammasome has been found to drive clonal expansion and pyroptotic cell
313 death in myelodysplastic syndromes (Basiorka et al., 2016). Our results demonstrate
314 that although the inflammasome is dispensable for HSPC emergence in zebrafish, it
315 cell-intrinsically regulates HSPC differentiation in homeostasis conditions at two

316 different levels: erythroid vs. myeloid cell fate decision and terminal erythroid
317 differentiation. Although CASP1 may target several proteins to regulate both processes,
318 one plausible scenario is the cleavage of GATA1 at residue D300 by CASP1, which
319 would result in the quick degradation of GATA1, since we were unable to detect
320 processed GATA1 in zebrafish larvae or K562 cells. The rapid induction of GATA1
321 protein amounts in mouse HSC upon pharmacological inhibition of CASP1 supports
322 this hypothesis. Although SPI1 protein amounts were unaffected by CASP1 inhibition
323 in HSC, SPI1 expression will be reduced at later stages of differentiation, but as a
324 consequence of reduced GM differentiation, not as a reason for it (Strasser et al., 2018).
325 Our model is compatible with our recent report showing that the expression of SPI1 is
326 not relevant for the erythroid vs. myeloid switch, since sometimes is already
327 downregulated or off when GATA1 expression starts but sometimes is still expressed
328 (Hoppe et al., 2016; Strasser et al., 2018). However, once GATA1 starts to be
329 expressed, the HSPC always differentiate into MegE with GATA1 high and SPI1 low or
330 off (Hoppe et al., 2016). Therefore, reduced GATA1 amounts upon inflammasome
331 activation lead to reduced erythropoiesis and thus increased myelopoiesis. At the same
332 time, inflammatory signaling through TNF and IL1b has recently been shown to
333 directly upregulate SPI1 protein directly in HSCs in vitro and *in vivo* (Etzrodt et al.,
334 2018; Pietras et al., 2016).

335 Similarly, terminal erythroid differentiation also requires GATA1 cleavage by
336 CASP1. Thus, we observed that pharmacological inhibition of CASP1 leads to GATA1
337 accumulation and altered erythroid differentiation of K562 cells. This is not unexpected,
338 since GATA1 inhibits terminal erythroid differentiation *in vitro* (Whyatt et al., 1997)
339 and *in vivo* (Whyatt et al., 2000). Although it remains to be elucidated the signals
340 responsible for the activation of the inflammasome in erythroid vs. myeloid cell fate
341 decision and terminal erythroid differentiation as well as the inflammasome components
342 involved, our genetic studies in zebrafish show that Gbp4 and Asc are both intrinsically
343 required *in vivo* by HSPC to regulate their differentiation. A mild activation of CASP1
344 is anticipated to avoid the pyroptotic cell death of hematopoietic cells. This may be
345 achieved by the assembly of small ASC specks and/or the low abundance of caspase-1
346 in hematopoietic progenitor cells and erythroid precursors, as occurs in neutrophils that
347 exhibit sustained interleukin-1 β (IL-1 β) release without pyroptosis compared to
348 macrophages (Boucher et al., 2018; Chen et al., 2014).

349 Hematopoietic lineage bias is associated to increased incidence of diseases with
350 prominent inflammatory components, including atherosclerosis, autoimmunity,
351 neurodegenerative disease and carcinogenesis (Elias et al., 2017). In particular,
352 neutrophilic dermatosis is characterized by the accumulation of neutrophils in the skin
353 and cutaneous lesions (Marzano et al., 2018). We observed that the robust neutrophilia
354 of a zebrafish model of skin inflammation is reversed by pharmacological inhibition of
355 Caspa, despite skin lesions and neutrophil infiltration are largely unaffected. Therefore,
356 inflammasome activation alters granulopoiesis through altered Gata1 expression and,
357 more importantly, its pharmacological inhibition restores the Gata1 regulation and
358 neutrophil counts. Furthermore, the critical role of the inflammasome in the regulation
359 of Gata1 has also been pointed out by the ability of pharmacological inhibition of Caspa
360 to restore erythroid hemoglobin and Gata1 amounts, and to decline Spi1 amounts, in a
361 zebrafish model of reduced Gata1, as occurs in Diamond-Blackfan anemia (Danilova
362 and Gazda, 2015). Collectively, all these results point out to the ability of
363 inflammasome inhibition as a therapeutic approach to treat human diseases with
364 associated hematopoietic lineage bias, such as neutrophilic inflammation (Marzano et
365 al., 2018; Ray and Kolls, 2017), ACD(Weiss, 2015) and chemotherapy-induced anemia
366 (Testa et al., 2015). The availability of an orally active CASP1 inhibitor, VX-765, with
367 high specificity, excellent pharmacokinetic properties and efficacy in rheumatoid
368 arthritis and skin inflammation mouse models (Wannamaker et al., 2007), further
369 supports the clinical testing of CASP1 inhibitors in hematopoietic lineage bias
370 disorders.

371

372 **Acknowledgments**

373 We strongly acknowledge I. Fuentes and P. Martínez for their excellent
374 technical assistance with the zebrafish experiments. We also thank Profs. S.A.
375 Renshaw, P. Crosier, G. Lieschke, M. Hammerschmidt, and M. Halpern for the
376 zebrafish lines, N. Inohara for the zebrafish Asc-Myc and Caspa constructs, C. Hall for
377 the zebrafish Gcsfa construct, D. Holden for the ST strain, and P. Pelegrín and A.
378 Baroja-Mazo for critical reading of the manuscript.

379

380 **Funding**

381 This work was supported by the Spanish Ministry of Science, Innovation and
382 Universities (grants BIO2014-52655-R and BIO2017-84702-R to VM and PI13/0234 to

383 MLC, PhD fellowship to FJMM and Juan de la Cierva postdoctoral contract to FAP), all
384 co-funded with Fondos Europeos de Desarrollo Regional/European Regional
385 Development Funds), Fundación Séneca-Murcia (grant 19400/PI/14 to MLC), the
386 University of Murcia (postdoctoral contracts to ABPO and DGM, and PhD fellowship
387 to FJMM), SNF grant 179490 to TS, and the European 7th Framework Initial Training
388 Network FishForPharma (PhD fellowship to SDT, PITG-GA-2011-289209). The
389 funders had no role in study design, data collection and analysis, decision to publish, or
390 preparation of the manuscript.

391

392 **Author contributions**

393 VM conceived the study; SDT, ABPO, CL, TS, LIZ, MLC, DGM and VM designed
394 research; SDT, ABPO, LRR, FJMM, FAP, FJMN, CL, NA, IPS, SC, ALM, AC, MPR
395 and DGM performed research; SDT, ABPO, LRR, FJMM, FAP, FJMN, CL, NA, TS,
396 IPS, SC, ALM, AC, MPR, LIZ, MLC, DGM and VM analyzed data; and SDT and VM
397 wrote the manuscript with minor contribution from other authors.

398

399 **Conflict of interest**

400 L.I.Z. is a founder and stockholder of Fate Therapeutics, Inc., Scholar Rock and Camp4
401 Therapeutics. A patent for the use of caspase-1 inhibitors to treat anemia has been
402 registered by Universidad de Murcia, Boston Children's Hospital and Instituto
403 Murciano de Investigación Biosanitaria (#P201831288).

404

405 **References**

406

- 407 Andersson, L.C., Nilsson, K., and Gahmberg, C.G. (1979). K562--a human
408 erythroleukemic cell line. *Int J Cancer* 23, 143-147.
- 409 Angosto, D., Lopez-Castejon, G., Lopez-Munoz, A., Sepulcre, M.P., Arizcun, M.,
410 Meseguer, J., and Mulero, V. (2012). Evolution of inflammasome functions in
411 vertebrates: Inflammasome and caspase-1 trigger fish macrophage cell death but
412 are dispensable for the processing of IL-1beta. *Innate Immun* 18, 815-824.
- 413 Basiorka, A.A., McGraw, K.L., Eksioglu, E.A., Chen, X., Johnson, J., Zhang, L.,
414 Zhang, Q., Irvine, B.A., Cluzeau, T., Sallman, D.A., *et al.* (2016). The NLRP3
415 inflammasome functions as a driver of the myelodysplastic syndrome phenotype.
416 *Blood* 128, 2960-2975.
- 417 Berman, J., Payne, E., and Hall, C. (2012). The zebrafish as a tool to study
418 hematopoiesis, human blood diseases, and immune function. *Adv Hematol* 2012,
419 425345.
- 420 Birbrair, A., and Frenette, P.S. (2016). Niche heterogeneity in the bone marrow. *Ann N*
421 *Y Acad Sci* 1370, 82-96.

422 Boucher, D., Monteleone, M., Coll, R.C., Chen, K.W., Ross, C.M., Teo, J.L., Gomez,
423 G.A., Holley, C.L., Bierschenk, D., Stacey, K.J., *et al.* (2018). Caspase-1 self-
424 cleavage is an intrinsic mechanism to terminate inflammasome activity. *J Exp Med*
425 *215*, 827-840.

426 Broz, P., and Monack, D.M. (2011). Molecular mechanisms of inflammasome
427 activation during microbial infections. *Immunol Rev* *243*, 174-190.

428 Burger, A., Lindsay, H., Felker, A., Hess, C., Anders, C., Chiavacci, E., Zaugg, J.,
429 Weber, L.M., Catena, R., Jinek, M., *et al.* (2016). Maximizing mutagenesis with
430 solubilized CRISPR-Cas9 ribonucleoprotein complexes. *Development* *143*, 2025-
431 2037.

432 Burns, C.E., Traver, D., Mayhall, E., Shepard, J.L., and Zon, L.I. (2005). Hematopoietic
433 stem cell fate is established by the Notch-Runx pathway. *Genes Dev* *19*, 2331-
434 2342.

435 Cabezas-Wallscheid, N., Klimmeck, D., Hansson, J., Lipka, D.B., Reyes, A., Wang, Q.,
436 Weichenhan, D., Lier, A., von Paleske, L., Renders, S., *et al.* (2014). Identification
437 of regulatory networks in HSCs and their immediate progeny via integrated
438 proteome, transcriptome, and DNA methylome analysis. *Cell Stem Cell* *15*, 507-
439 522.

440 Cantor, A.B., and Orkin, S.H. (2002). Transcriptional regulation of erythropoiesis: an
441 affair involving multiple partners. *Oncogene* *21*, 3368-3376.

442 Carney, T.J., von der Hardt, S., Sonntag, C., Amsterdam, A., Topczewski, J., Hopkins,
443 N., and Hammerschmidt, M. (2007). Inactivation of serine protease Matrilysin1
444 by its inhibitor Hai1 is required for epithelial integrity of the zebrafish epidermis.
445 *Development* *134*, 3461-3471.

446 Chen, K.W., Gross, C.J., Sotomayor, F.V., Stacey, K.J., Tschopp, J., Sweet, M.J., and
447 Schroder, K. (2014). The neutrophil NLRC4 inflammasome selectively promotes
448 IL-1beta maturation without pyroptosis during acute Salmonella challenge. *Cell*
449 *Rep* *8*, 570-582.

450 Cumano, A., and Godin, I. (2007). Ontogeny of the hematopoietic system. *Annu Rev*
451 *Immunol* *25*, 745-785.

452 Curado, S., Anderson, R.M., Jungblut, B., Mumm, J., Schroeter, E., and Stainier, D.Y.
453 (2007). Conditional targeted cell ablation in zebrafish: a new tool for regeneration
454 studies. *Dev Dyn* *236*, 1025-1035.

455 Curado, S., Stainier, D.Y., and Anderson, R.M. (2008). Nitroreductase-mediated
456 cell/tissue ablation in zebrafish: a spatially and temporally controlled ablation
457 method with applications in developmental and regeneration studies. *Nat Protoc* *3*,
458 948-954.

459 Danilova, N., and Gazda, H.T. (2015). Ribosomopathies: how a common root can cause
460 a tree of pathologies. *Dis Model Mech* *8*, 1013-1026.

461 Davison, J.M., Akitake, C.M., Goll, M.G., Rhee, J.M., Gosse, N., Baier, H., Halpern,
462 M.E., Leach, S.D., and Parsons, M.J. (2007). Transactivation from Gal4-VP16
463 transgenic insertions for tissue-specific cell labeling and ablation in zebrafish. *Dev*
464 *Biol* *304*, 811-824.

465 De Maria, R., Zeuner, A., Eramo, A., Domenichelli, C., Bonci, D., Grignani, F.,
466 Srinivasula, S.M., Alnemri, E.S., Testa, U., and Peschle, C. (1999). Negative
467 regulation of erythropoiesis by caspase-mediated cleavage of GATA-1. *Nature* *401*,
468 489-493.

469 de Oliveira, S., Reyes-Aldasoro, C.C., Candel, S., Renshaw, S.A., Mulero, V., and
470 Calado, A. (2013). Cxcl8 (IL-8) mediates neutrophil recruitment and behavior in
471 the zebrafish inflammatory response. *J Immunol* *190*, 4349-4359.

472 Elias, H.K., Bryder, D., and Park, C.Y. (2017). Molecular mechanisms underlying
473 lineage bias in aging hematopoiesis. *Semin Hematol* 54, 4-11.

474 Ellett, F., and Lieschke, G.J. (2010). Zebrafish as a model for vertebrate hematopoiesis.
475 *Curr Opin Pharmacol* 10, 563-570.

476 Ellett, F., Pase, L., Hayman, J.W., Andrianopoulos, A., and Lieschke, G.J. (2011).
477 mpeg1 promoter transgenes direct macrophage-lineage expression in zebrafish.
478 *Blood* 117, e49-56.

479 Espin-Palazon, R., Weijts, B., Mulero, V., and Traver, D. (2018). Proinflammatory
480 Signals as Fuel for the Fire of Hematopoietic Stem Cell Emergence. *Trends Cell*
481 *Biol* 28, 58-66.

482 Etzrodt, M., Ahmed, N., Hoppe, P.S., Loeffler, D., Skylaki, S., Hilsenbeck, O.,
483 Kokkaliaris, K.D., Kaltenbach, H.M., Stelling, J., Nerlov, C., and Schroeder, T.
484 (2018). Inflammatory signals directly instruct PU.1 in HSCs via TNF. *Blood*.

485 Ferreira, R., Ohneda, K., Yamamoto, M., and Philipsen, S. (2005). GATA1 function, a
486 paradigm for transcription factors in hematopoiesis. *Mol Cell Biol* 25, 1215-1227.

487 Ganis, J.J., Hsia, N., Trompouki, E., de Jong, J.L., DiBiase, A., Lambert, J.S., Jia, Z.,
488 Sabo, P.J., Weaver, M., Sandstrom, R., *et al.* (2012). Zebrafish globin switching
489 occurs in two developmental stages and is controlled by the LCR. *Dev Biol* 366,
490 185-194.

491 Gore, A.V., Pillay, L.M., Venero Galanternik, M., and Weinstein, B.M. (2018). The
492 zebrafish: A fintastic model for hematopoietic development and disease. *Wiley*
493 *Interdiscip Rev Dev Biol* 7, e312.

494 Hall, C., Flores, M.V., Storm, T., Crosier, K., and Crosier, P. (2007). The zebrafish
495 lysozyme C promoter drives myeloid-specific expression in transgenic fish. *BMC*
496 *Dev Biol* 7, 42.

497 Hall, C.J., Flores, M.V., Oehlers, S.H., Sanderson, L.E., Lam, E.Y., Crosier, K.E., and
498 Crosier, P.S. (2012). Infection-responsive expansion of the hematopoietic stem and
499 progenitor cell compartment in zebrafish is dependent upon inducible nitric oxide.
500 *Cell Stem Cell* 10, 198-209.

501 Halpern, M.E., Rhee, J., Goll, M.G., Akitake, C.M., Parsons, M., and Leach, S.D.
502 (2008). Gal4/UAS transgenic tools and their application to zebrafish. *Zebrafish* 5,
503 97-110.

504 Hilsenbeck, O., Schwarzfischer, M., Loeffler, D., Dimopoulos, S., Hastreiter, S., Marr,
505 C., Theis, F.J., and Schroeder, T. (2017). fastER: a user-friendly tool for ultrafast
506 and robust cell segmentation in large-scale microscopy. *Bioinformatics* 33, 2020-
507 2028.

508 Hilsenbeck, O., Schwarzfischer, M., Skylaki, S., Schauburger, B., Hoppe, P.S., Loeffler,
509 D., Kokkaliaris, K.D., Hastreiter, S., Skylaki, E., Filipczyk, A., *et al.* (2016).
510 Software tools for single-cell tracking and quantification of cellular and molecular
511 properties. *Nat Biotechnol* 34, 703-706.

512 Hoppe, P.S., Schwarzfischer, M., Loeffler, D., Kokkaliaris, K.D., Hilsenbeck, O.,
513 Moritz, N., Endele, M., Filipczyk, A., Gambardella, A., Ahmed, N., *et al.* (2016).
514 Early myeloid lineage choice is not initiated by random PU.1 to GATA1 protein
515 ratios. *Nature* 535, 299-302.

516 Jagannathan-Bogdan, M., and Zon, L.I. (2013). Hematopoiesis. *Development* 140,
517 2463-2467.

518 Kiel, M.J., Yilmaz, O.H., Iwashita, T., Yilmaz, O.H., Terhorst, C., and Morrison, S.J.
519 (2005). SLAM family receptors distinguish hematopoietic stem and progenitor
520 cells and reveal endothelial niches for stem cells. *Cell* 121, 1109-1121.

521 Koeffler, H.P., and Golde, D.W. (1980). Human myeloid leukemia cell lines: a review.
522 *Blood* 56, 344-350.

523 Kondo, M. (2010). Lymphoid and myeloid lineage commitment in multipotent
524 hematopoietic progenitors. *Immunol Rev* 238, 37-46.

525 Kondo, M., Wagers, A.J., Manz, M.G., Prohaska, S.S., Scherer, D.C., Beilhack, G.F.,
526 Shizuru, J.A., and Weissman, I.L. (2003). Biology of hematopoietic stem cells and
527 progenitors: implications for clinical application. *Annu Rev Immunol* 21, 759-806.

528 Kuri, P., Schieber, N.L., Thumberger, T., Wittbrodt, J., Schwab, Y., and Leptin, M.
529 (2017). Dynamics of in vivo ASC speck formation. *J Cell Biol* 216, 2891-2909.

530 Kwan, K.M., Fujimoto, E., Grabher, C., Mangum, B.D., Hardy, M.E., Campbell, D.S.,
531 Parant, J.M., Yost, H.J., Kanki, J.P., and Chien, C.B. (2007). The Tol2kit: a
532 multisite gateway-based construction kit for Tol2 transposon transgenesis
533 constructs. *Dev Dyn* 236, 3088-3099.

534 Lamkanfi, M., and Dixit, V.M. (2014). Mechanisms and functions of inflammasomes.
535 *Cell* 157, 1013-1022.

536 Latz, E., Xiao, T.S., and Stutz, A. (2013). Activation and regulation of the
537 inflammasomes. *Nat Rev Immunol* 13, 397-411.

538 Le Guyader, D., Redd, M.J., Colucci-Guyon, E., Murayama, E., Kissa, K., Briolat, V.,
539 Mordelet, E., Zapata, A., Shinomiya, H., and Herbomel, P. (2008). Origins and
540 unconventional behavior of neutrophils in developing zebrafish. *Blood* 111, 132-
541 141.

542 Liongue, C., Hall, C.J., O'Connell, B.A., Crosier, P., and Ward, A.C. (2009). Zebrafish
543 granulocyte colony-stimulating factor receptor signaling promotes myelopoiesis
544 and myeloid cell migration. *Blood* 113, 2535-2546.

545 Lopez-Castejon, G., Sepulcre, M.P., Mulero, I., Pelegrin, P., Meseguer, J., and Mulero,
546 V. (2008). Molecular and functional characterization of gilthead seabream *Sparus*
547 *aurata* caspase-1: the first identification of an inflammatory caspase in fish. *Mol*
548 *Immunol* 45, 49-57.

549 Martinon, F., Mayor, A., and Tschopp, J. (2009). The inflammasomes: guardians of the
550 body. *Annu Rev Immunol* 27, 229-265.

551 Marzano, A.V., Borghi, A., Wallach, D., and Cugno, M. (2018). A Comprehensive
552 Review of Neutrophilic Diseases. *Clin Rev Allergy Immunol* 54, 114-130.

553 Masters, S.L., Gerlic, M., Metcalf, D., Preston, S., Pellegrini, M., O'Donnell, J.A.,
554 McArthur, K., Baldwin, T.M., Chevrier, S., Nowell, C.J., *et al.* (2012). NLRP1
555 inflammasome activation induces pyroptosis of hematopoietic progenitor cells.
556 *Immunity* 37, 1009-1023.

557 Masumoto, J., Zhou, W., Chen, F.F., Su, F., Kuwada, J.Y., Hidaka, E., Katsuyama, T.,
558 Sagara, J., Taniguchi, S., Ngo-Hazelett, P., *et al.* (2003). Caspy, a zebrafish
559 caspase, activated by ASC oligomerization is required for pharyngeal arch
560 development. *J Biol Chem* 278, 4268-4276.

561 Mathias, J.R., Dodd, M.E., Walters, K.B., Rhodes, J., Kanki, J.P., Look, A.T., and
562 Huttenlocher, A. (2007). Live imaging of chronic inflammation caused by mutation
563 of zebrafish *Hai1*. *J Cell Sci* 120, 3372-3383.

564 Morrison, S.J., Shah, N.M., and Anderson, D.J. (1997). Regulatory mechanisms in stem
565 cell biology. *Cell* 88, 287-298.

566 Nerlov, C., Querfurth, E., Kulesa, H., and Graf, T. (2000). GATA-1 interacts with the
567 myeloid PU.1 transcription factor and represses PU.1-dependent transcription.
568 *Blood* 95, 2543-2551.

569 Pfaffl, M.W. (2001). A new mathematical model for relative quantification in real-time
570 RT-PCR. *Nucleic Acids Res* 29, e45.

571 Pietras, E.M., Mirantes-Barbeito, C., Fong, S., Loeffler, D., Kovtonyuk, L.V., Zhang,
572 S., Lakshminarasimhan, R., Chin, C.P., Techner, J.M., Will, B., *et al.* (2016).
573 Chronic interleukin-1 exposure drives haematopoietic stem cells towards
574 precocious myeloid differentiation at the expense of self-renewal. *Nat Cell Biol* 18,
575 607-618.

576 Pilla, D.M., Hagar, J.A., Haldar, A.K., Mason, A.K., Degrandi, D., Pfeffer, K., Ernst,
577 R.K., Yamamoto, M., Miao, E.A., and Coers, J. (2014). Guanylate binding proteins
578 promote caspase-11-dependent pyroptosis in response to cytoplasmic LPS. *Proc*
579 *Natl Acad Sci U S A* 111, 6046-6051.

580 Prajsnar, T.K., Hamilton, R., Garcia-Lara, J., McVicker, G., Williams, A., Boots, M.,
581 Foster, S.J., and Renshaw, S.A. (2012). A privileged intraphagocyte niche is
582 responsible for disseminated infection of *Staphylococcus aureus* in a zebrafish
583 model. *Cell Microbiol* 14, 1600-1619.

584 Rathinam, V.A., and Fitzgerald, K.A. (2016). Inflammasome Complexes: Emerging
585 Mechanisms and Effector Functions. *Cell* 165, 792-800.

586 Ray, A., and Kolls, J.K. (2017). Neutrophilic Inflammation in Asthma and Association
587 with Disease Severity. *Trends Immunol* 38, 942-954.

588 Rekhtman, N., Radparvar, F., Evans, T., and Skoultschi, A.I. (1999). Direct interaction
589 of hematopoietic transcription factors PU.1 and GATA-1: functional antagonism in
590 erythroid cells. *Genes Dev* 13, 1398-1411.

591 Renshaw, S.A., Loynes, C.A., Trushell, D.M., Elworthy, S., Ingham, P.W., and Whyte,
592 M.K. (2006). A transgenic zebrafish model of neutrophilic inflammation. *Blood*
593 108, 3976-3978.

594 Santos, J.C., Dick, M.S., Lagrange, B., Degrandi, D., Pfeffer, K., Yamamoto, M.,
595 Meunier, E., Pelczar, P., Henry, T., and Broz, P. (2018). LPS targets host
596 guanylate-binding proteins to the bacterial outer membrane for non-canonical
597 inflammasome activation. *EMBO J* 37.

598 Schindelin, J., Arganda-Carreras, I., Frise, E., Kaynig, V., Longair, M., Pietzsch, T.,
599 Preibisch, S., Rueden, C., Saalfeld, S., Schmid, B., *et al.* (2012). Fiji: an open-
600 source platform for biological-image analysis. *Nat Methods* 9, 676-682.

601 Sharma, D., and Kanneganti, T.D. (2016). The cell biology of inflammasomes:
602 Mechanisms of inflammasome activation and regulation. *J Cell Biol* 213, 617-629.

603 Smith, R.D., Malley, J.D., and Schechter, A.N. (2000). Quantitative analysis of globin
604 gene induction in single human erythroleukemic cells. *Nucleic Acids Res* 28, 4998-
605 5004.

606 Stachura, D.L., Svoboda, O., Campbell, C.A., Espin-Palazon, R., Lau, R.P., Zon, L.I.,
607 Bartunek, P., and Traver, D. (2013). The zebrafish granulocyte colony-stimulating
608 factors (Gcsfs): 2 paralogous cytokines and their roles in hematopoietic
609 development and maintenance. *Blood* 122, 3918-3928.

610 Strasser, M.K., Hoppe, P.S., Loeffler, D., Kokkaliaris, K.D., Schroeder, T., Theis, F.J.,
611 and Marr, C. (2018). Lineage marker synchrony in hematopoietic genealogies
612 refutes the PU.1/GATA1 toggle switch paradigm. *Nat Commun* 9, 2697.

613 Tamplin, O.J., Durand, E.M., Carr, L.A., Childs, S.J., Hagedorn, E.J., Li, P., Yzaguirre,
614 A.D., Speck, N.A., and Zon, L.I. (2015). Hematopoietic stem cell arrival triggers
615 dynamic remodeling of the perivascular niche. *Cell* 160, 241-252.

616 Testa, U., Castelli, G., and Elvira, P. (2015). Experimental and investigational therapies
617 for chemotherapy-induced anemia. *Expert Opin Investig Drugs* 24, 1433-1445.

618 Thisse, C., Thisse, B., Schilling, T.F., and Postlethwait, J.H. (1993). Structure of the
619 zebrafish *snail1* gene and its expression in wild-type, spadetail and no tail mutant
620 embryos. *Development* 119, 1203-1215.

621 Tyrkalska, S.D., Candel, S., Angosto, D., Gomez-Abellan, V., Martin-Sanchez, F.,
622 Garcia-Moreno, D., Zapata-Perez, R., Sanchez-Ferrer, A., Sepulcre, M.P., Pelegrin,
623 P., and Mulero, V. (2016). Neutrophils mediate Salmonella Typhimurium
624 clearance through the GBP4 inflammasome-dependent production of
625 prostaglandins. *Nat Commun* 7, 12077.

626 Tyrkalska, S.D., Candel, S., Perez-Oliva, A.B., Valera, A., Alcaraz-Perez, F., Garcia-
627 Moreno, D., Cayuela, M.L., and Mulero, V. (2017). Identification of an
628 Evolutionarily Conserved Ankyrin Domain-Containing Protein, Caiap, Which
629 Regulates Inflammasome-Dependent Resistance to Bacterial Infection. *Front*
630 *Immunol* 8, 1375.

631 Wallet, P., Benaoudia, S., Mosnier, A., Lagrange, B., Martin, A., Lindgren, H.,
632 Golovliov, I., Michal, F., Basso, P., Djebali, S., *et al.* (2017). IFN-gamma extends
633 the immune functions of Guanylate Binding Proteins to inflammasome-
634 independent antibacterial activities during Francisella novicida infection. *PLoS*
635 *Pathog* 13, e1006630.

636 Wannamaker, W., Davies, R., Namchuk, M., Pollard, J., Ford, P., Ku, G., Decker, C.,
637 Charifson, P., Weber, P., Germann, U.A., *et al.* (2007). (S)-1-((S)-2- $\{[1-(4\text{-amino-}$
638 $3\text{-chloro-phenyl)-methanoyl]-amino}\}$ -3,3-dimethyl-butanoyl)-pyrrolidine-2-
639 $\text{-carboxylic acid ((2R,3S)-2-ethoxy-5-oxo-tetrahydro-furan-3-yl)-amide (VX-765)}$,
640 an orally available selective interleukin (IL)-converting enzyme/caspase-1
641 inhibitor, exhibits potent anti-inflammatory activities by inhibiting the release of
642 IL-1beta and IL-18. *J Pharmacol Exp Ther* 321, 509-516.

643 Weiss, G. (2015). Anemia of Chronic Disorders: New Diagnostic Tools and New
644 Treatment Strategies. *Semin Hematol* 52, 313-320.

645 Weissman, I.L. (2000). Translating stem and progenitor cell biology to the clinic:
646 barriers and opportunities. *Science* 287, 1442-1446.

647 Westerfield, M. (2000). *The Zebrafish Book. A Guide for the Laboratory Use of*
648 *Zebrafish Danio* (Brachydanio) rerio.* (Eugene, OR.: University of Oregon Press.).

649 White, R.M., Sessa, A., Burke, C., Bowman, T., LeBlanc, J., Ceol, C., Bourque, C.,
650 Dovey, M., Goessling, W., Burns, C.E., and Zon, L.I. (2008). Transparent adult
651 zebrafish as a tool for in vivo transplantation analysis. *Cell Stem Cell* 2, 183-189.

652 Whyatt, D., Lindeboom, F., Karis, A., Ferreira, R., Milot, E., Hendriks, R., de Bruijn,
653 M., Langeveld, A., Gribnau, J., Grosveld, F., and Philipsen, S. (2000). An intrinsic
654 but cell-nonautonomous defect in GATA-1-overexpressing mouse erythroid cells.
655 *Nature* 406, 519-524.

656 Whyatt, D.J., Karis, A., Harkes, I.C., Verkerk, A., Gillemans, N., Elefanty, A.G., Vairo,
657 G., Ploemacher, R., Grosveld, F., and Philipsen, S. (1997). The level of the tissue-
658 specific factor GATA-1 affects the cell-cycle machinery. *Genes Funct* 1, 11-24.

659 Wu, W.C., Sun, H.W., Chen, H.T., Liang, J., Yu, X.J., Wu, C., Wang, Z., and Zheng, L.
660 (2014). Circulating hematopoietic stem and progenitor cells are myeloid-biased in
661 cancer patients. *Proc Natl Acad Sci U S A* 111, 4221-4226.

662 Yang, L., Wang, L., Kalfa, T.A., Cancelas, J.A., Shang, X., Pushkaran, S., Mo, J.,
663 Williams, D.A., and Zheng, Y. (2007). Cdc42 critically regulates the balance
664 between myelopoiesis and erythropoiesis. *Blood* 110, 3853-3861.

665 Zwack, E.E., Feeley, E.M., Burton, A.R., Hu, B., Yamamoto, M., Kanneganti, T.D.,
666 Bliska, J.B., Coers, J., and Brodsky, I.E. (2017). Guanylate Binding Proteins
667 Regulate Inflammasome Activation in Response to Hyperinjected Yersinia
668 Translocon Components. *Infect Immun* 85.

669
670

671 **Figure Legends**

672

673 **Figure 1. Inflammasome inhibition results in decreased neutrophil but increased**
674 **erythrocyte numbers in zebrafish.** *Tg(mpx:eGFP)* (A-J) and *Tg(lcr:eGFP)* (L)
675 zebrafish one-cell embryos were injected with standard control (Std), Asc or Gbp4 MOs
676 (A, B, G, H, K), and/or with antisense (As), Gbp4^{WT}, Gbp4^{KS/AA}, Gbp4^{ΔCARD}, Gbp4^{DM},
677 Asc or Caspa mRNAs (e-h). Alternatively, *Tg(mpx:eGFP)* (C, D, I, J) and
678 *Tg(lcr:eGFP)* (K) embryos left uninjected were manually dechorionated at 24 or 48 hpf
679 and treated by immersion with DMSO or the irreversible caspase-1 inhibitor Ac-
680 YVAD-CMK (C1INH). Each dot represents the number of neutrophils (A, C, E, G, I)
681 from a single larva or the percentage of erythrocytes from each pool of 50 larvae (K, L),
682 while the mean ± SEM for each group is also shown. The sample size (n) is indicated
683 for each treatment. Representative images of green channels of whole larvae for the
684 different treatments are also shown. Scale bars, 500 μm. Caspase-1 activity in whole
685 larvae was determined for each treatment at 72 hpf (one representative caspase-1
686 activity assay out of the three carried out is shown) (B, D, F, H, J). *p<0.05; **p<0.01;
687 ***p<0.001 according to ANOVA followed by Tukey multiple range test. See also
688 Figures S1-S4.

689

690 **Figure 2. The inflammasome is intrinsically required for HSC differentiation but is**
691 **dispensable for their emergence in zebrafish.** (A-H) *Tg(runx1:GAL4; UAS:nfsb-*
692 *mCherry)* zebrafish embryos were manually dechorionated at 24 or 48 hpf and treated
693 by immersion with DMSO or the irreversible caspase-1 inhibitor Ac-YVAD-CMK
694 (C1INH) for 24 or 48 h (A-F). Alternatively, *Tg(runx1:GAL4; UAS:nfsb-mCherry)* one-
695 cell embryos were injected with standard control (Std) or Asc MOs (G-H). Each dot
696 represents the number of HSCs from a single larva, while the mean ± SEM for each
697 group is also shown. The sample size (n) is indicated for each treatment. Representative
698 images of red channels of whole larvae for the different treatments are also shown (A,
699 C, E, G). Scale bars, 500 μm. Caspase-1 activity was determined for each treatment
700 from 48 or 72 hpf larvae (one representative caspase-1 activity assay out of the three
701 carried out is shown) (B, D, F, H). (I-L) *Tg(runx1:gal4; UAS:Gbp4KS/AA)* (I),
702 *Tg(mpx:gal4; UAS:Gbp4KS/AA)* (J), *Tg(runx1:gal4; UAS:AscΔCARD)* (K),
703 *Tg(mpx:gal4; UAS:AscΔCARD)* (L) larvae were fixed at 72 hpf and stained with Sudan
704 black for the detection of neutrophils. Each dot represents the number of neutrophils

705 from a single larva, while the mean \pm SEM for each group is also shown. The sample
706 size (n) is indicated for each treatment. ns, not significant; * $p < 0.05$; ** $p < 0.01$;
707 *** $p < 0.001$ according to Student *t* test. See also Figure S4.

708

709 **Figure 3. Inflammasome activity is indispensable for myelopoiesis in zebrafish.**
710 *Tg(mpx:GAL4; UAS:nsfb-mCherry)* zebrafish larvae were manually dechorionated at 48
711 hpf and treated by immersion with metronidazole (Mtz) for 24 h and then with DMSO
712 or the irreversible caspase-1 inhibitor Ac-YVAD-CMK (C1INH) for the next 4 days.
713 Control groups were treated for 5 days with Mtz (all time). (A) Each dot represents the
714 number of neutrophils from a single larva, while the mean \pm SEM for each group is also
715 shown. (B) Representative images of red channels of whole larvae for the different
716 treatments and time points are also shown. Scale bars, 500 μm . *** $p < 0.001$ according
717 to ANOVA followed by Tukey multiple range test.

718

719 **Figure 4. Infection is unable to bypass the inflammasome requirement for**
720 **neutrophil production in zebrafish.** (A-H). *Tg(mpx:eGFP)* zebrafish one-cell embryos
721 were injected with standard control (Std), Gbp4 or Asc MOs in combination with
722 antisense (As), Gcsfa, Asc, Caspa mRNAs (C, D, G, H-J) or left uninjected, manually
723 dechorionated at 48 hpf and treated by immersion with DMSO or the irreversible
724 caspase-1 inhibitor Ac-YVAD-CMK (C1INH) (A, B, E, F). Larvae were then infected
725 at 48 hpf with *S. Typhimurium* (S.I.) in the otic vesicle (A, B) or the yolk sac (G, H)
726 and the number of neutrophils was counted in the whole body at 24 hpi (A, B) or 72 hpf
727 (C-F) and the survival was determined during 5 days after the infection (G, H). Each dot
728 represents the number of neutrophils from a single larva, while the mean \pm SEM for
729 each group is also shown. The sample size (n) is indicated for each treatment. Note that
730 the 4 non-infected group showed no mortality and the 4 lines are overlapping.
731 Representative images of green channels of whole larvae for the different treatments are
732 shown (A-F). Scale bars, 500 μm . Caspase-1 activity was determined in whole larvae
733 for each treatment at 72 hpf (one representative caspase-1 activity assay out of the three
734 carried out is shown) (B, D, F). (I-J) The mRNA amounts of *spilb*, *gatala*, *mcsf* and
735 *gcsf* in larval tails were measured by RT-qPCR at 24 hpf (I), while the protein amounts
736 of Gatala and histone H3 were determined using western blot in larval tails at 24 hpf
737 (J). A densitometry analysis was performed to check the differences between
738 treatments. ns, not significant; * $p < 0.05$; ** $p < 0.01$; *** $p < 0.001$ according to ANOVA

739 followed by Tukey multiple range test (A-F, I, J) or log rank test with Bonferroni
740 correction (G, H).

741 **Figure 5. Inflammasome inhibition increases GATA1 protein amounts and**
742 **megakaryocyte-erythrocyte colony output in mouse HSCs.** (A) Flow cytometry
743 gating scheme used for isolation of mouse HSCs. HSCs are sorted as Lin-
744 cKit⁺Sca1⁺CD48⁻CD34⁻CD135⁻CD150⁺. Numbers in the plots indicate % of lineage
745 depleted BM cells. (B, C) Caspase1-inhibitor (C1INH) treatment increases Gata1
746 protein amounts (B) without affecting Spi1 protein amounts (C) in mouse HSCs. Data
747 were acquired by time-lapse imaging of freshly-sorted HSCs (DMSO=605, C1INH=749
748 HSCs) from 12-week old Spi1-eYFP and Gata1-mCherry fluorescent protein fusion
749 reporter mice in IMDM + BIT + SCF + Epo + Tpo + IL3 + IL6 supplemented with or
750 without 100 μ M of the irreversible caspase-1 inhibitor Ac-YVAD-CMK (2 biological
751 replicates). (D) Caspase1-inhibitor treatment increased MegE colony output at the
752 expense of GM colonies. HSCs from Spi1-eYFP and Gata1-mCherry reporter mice
753 were single-cell sorted into 384 well plates in IMDM + BIT + SCF + Epo + Tpo + IL3
754 + IL6 supplemented with or without 100 μ M Ac-YVAD-CMK. At day 8, color
755 conjugated CD41-APC and CD16/32-BV421 antibodies were added to the colonies and
756 colonies were imaged and manually scored using morphology, Spi1-eYFP and CD16/32
757 signal to indicate GM colonies and Gata1-mCherry and CD41 signal to indicate MegE
758 colonies. Data represent mean percentage of types of colonies formed from HSCs from
759 4 independent experiments (244 total colonies scored, Error bars = SEM). ns, not
760 significant; * p <0.05; ** p <0.01; *** p <0.001 according to two tailed Student's T-test (A,
761 B) and Chi-square test (C).

762

763 **Figure 6. Pharmacological inhibition of caspase-1 impairs erythroid differentiation**
764 **of K562 cells.** K562 cells were incubated with 50 μ M hemin for the indicated times in
765 the presence or absence of the irreversible caspase-1 inhibitor Ac-YVAD-CMK
766 (C1INH, 100 μ M) and the cell pellets imaged (A, E, F), lysed and resolved by SDS-
767 PAGE and immunoblotted with anti-GATA1 and anti-ACTB antibodies (A, E, F),
768 processed for the quantification of caspase-1 activity using the fluorogenic substrate
769 YVAD-AFC (B, G) and for immunofluorescence using anti-CASP1 (C) and anti-
770 GATA1 (D) antibodies. Cell extracts from HEK293T transfected with GATA1-FLAG
771 and empty FLAG were included as mobility controls in a. Nuclei were stained with

772 DAPI. One representative caspase-1 activity (B, G), western blot (A, E, F) and
773 hemoglobin accumulation (A, E, F) assay out of the three carried out is shown, while
774 one representative immunofluorescence staining (C, D) assay out of the two carried out
775 is shown. Scale bars, 5 μm . *** $p < 0.001$ according to ANOVA followed by Tukey
776 multiple range test. See also Figures S5-S7.

777

778 **Figure 7. Pharmacological inhibition of caspase-1 rescues zebrafish models of**
779 **neutrophilic inflammation and anemia.** (A-G) Wild type and *spint1a* mutant larvae
780 were manually dechorionated and treated from 1-3 dpf with the irreversible caspase-1
781 inhibitor Ac-YVAD-CMK (C1INH, 100 μM) (A-E) or one-cell embryos injected with
782 control (std) or *caspa* sgRNA and recombinant Cas9 (F, G). Caspase-1 activity (A), the
783 *spi1b/gata1a* gene expression ratio (B), neutrophil dispersion (C) and the number of
784 neutrophils (D-G) were then determined. Each dot represents the number of neutrophils
785 from a single larva, while the mean \pm SEM for each group is also shown. The sample
786 size (n) is indicated for each treatment. Representative overlay images of green and
787 bright field channels of whole larvae for the different treatments are shown (e, g). Scale
788 bar, 500 μm . (H-J) Zebrafish one-cell embryos were injected with standard control (Std)
789 or Gata1a MOs, manually dechorionated at 24 hpf and treated by immersion with
790 DMSO or the reversible caspase-1 inhibitor Ac-YVAD-CHO (C1INH) for 24-48 hpf.
791 The inhibitor was then washed off and the larvae incubated until 72 hpf. Representative
792 pictures of Gata1a-deficient larvae with mild, moderate and severe anemia (H),
793 quantification of the phenotype of larval treated with DMSO or C1INH (I) and
794 immunoblot of larval extracts with anti-Gata1a, anti-Spi1b and anti-Actb antibodies (J).
795 One representative caspase-1 activity (A) and western blot (J) assay out of the three and
796 two, respectively, carried out is shown. ns, not significant; * $p < 0.05$; ** $p < 0.01$;
797 *** $p < 0.001$ according to Student *t* test (A, B), ANOVA followed by Tukey multiple
798 range test (C, D, F) and Fisher's exact test (I).

799

800

801 **STAR Methods**

802

803 **Contact for Reagent and Resource Sharing**

804 Further information and requests for resources and reagents should be directed to and
805 will be fulfilled by the Lead Contact, Victoriano Mulero (vmulero@um.es).

806

807 **Experimental Model and Subject Details**

808 Zebrafish (*Danio rerio* H.) were obtained from the Zebrafish International
809 Resource Center and mated, staged, raised and processed as described (Westerfield,
810 2000). The lines *roy^{a9/a9}*; *nacre^{w2/w2}* (*casper*) (White et al., 2008), *Tg(mpx:eGFP)ⁱ¹¹⁴*
811 (Renshaw et al., 2006), *Tg(mpeg1:eGFP)^{g122}*, *Tg(mpeg1:GAL4)^{g125}* (Ellett et al., 2011),
812 *Tg(lyz:dsRED)^{nz50}* (Hall et al., 2007), *Tg(mpx:Gal4.VP16)ⁱ²²²* (Davison et al., 2007),
813 *Tg(lcr:eGFP)^{cz3325}* (Ganis et al., 2012), *Tg(runx1:GAL4)^{utm6}* (Tamplin et al., 2015),
814 *Tg(UAS:nfsB-mCherry)^{c264}* (Davison et al., 2007) and *Tg(spint1a)^{hi2217}* (Carney et al.,
815 2007; Mathias et al., 2007) have been previously described. The experiments performed
816 comply with the Guidelines of the European Union Council (Directive 2010/63/EU) and
817 the Spanish RD 53/2013. Experiments and procedures were performed as approved by
818 the Bioethical Committees of the University of Murcia (approval numbers #75/2014,
819 #216/2014 and 395/2017).

820 Mouse experiments were performed with 12-16 week old, male, Spi1-eYFP and
821 Gata-mCherry1 reporter mice (C57BL/6J background). Animal experiments were
822 approved according to Institutional guidelines of ETH Zurich and Swiss Federal Law by
823 veterinary office of Canton Basel-Stadt, Switzerland (approval number #2655).

824

825 **Method Details**

826 *DNA Construct and generation of transgenics*

827 The *uas:AscΔCARD-GFP* construct was generated by MultiSite Gateway
828 assemblies using LR Clonase II Plus (Life Technologies) according to standard
829 protocols and using Tol2kit vectors described previously (Kwan et al., 2007). The
830 expression constructs *Gbp4*, *Gbp4KS→AA*, *Gbp4ΔCARD*, *Gbp4KS→AA* and
831 *ΔCARD* (double mutant, DM) and *uas:gbp4KS/AA* (Tyrkalska et al., 2016); *Asc-Myc*
832 and *Caspa* (Masumoto et al., 2003); and *Gcsfa* (Liongue et al., 2009) were previously
833 described.

834 The line *Tg(UAS:gbp4KS/AA)^{ums3}* was previously described (Tyrkalska et al.,
835 2016). *Tg(UAS:ascΔCARD-GFP)^{ums4}* was generated by microinjecting 0.5-1 nl into the
836 yolk sac of one-cell-stage embryos a solution containing 100 ng/μl *uas:ascΔCARD-*
837 *GFP* and *uas:gbp4KS→AA* constructs, respectively, and 50 ng/μl Tol2 RNA in
838 microinjection buffer (×0.5 Tango buffer and 0.05% phenol red solution) using a
839 microinjector (Narishige).

840

841 *Morpholino, RNA and protein injection and chemical treatments of zebrafish larvae*

842 Specific morpholinos (Gene Tools) were resuspended in nuclease-free water at 1
843 mM (Table S1). *In vitro*-transcribed RNA was obtained following the manufacturer's
844 instructions (mMESSAGE mMACHINE kit, Ambion). Morpholinos and RNA were
845 mixed in microinjection buffer and microinjected into the yolk sac of one-cell-stage
846 embryos using a microinjector (Narishige) (0.5-1 nl per embryo). The same amount of
847 MOs and/or RNA was used in all experimental groups.

848 For genetic inactivation of *caspa*, injection mixes were prepared with 500 ng/μl
849 EnGen® Cas9 NLS from *Streptococcus pyogenes* (New England Biolabs) and 100
850 ng/μl control (5'-3') or *caspa* (5'-GAACCAATTCCGAAGGATCC-3') sgRNA in 300
851 mM KCl buffer, incubated for 5 min at 37°C and used directly without further storage
852 (Burger et al., 2016).

853 In some experiments, 1-2 dpf embryos were manually dechorionated and treated
854 for 1 to 3 dpf at 28°C by bath immersion with the caspase-1 inhibitors Ac-YVAD-CMK
855 (irreversible) or Ac-YVAD-CHO (reversible), and the reversible caspase-4 and caspase-
856 5 inhibitor Ac-LEVD-CHO (100 μM, Peptanova) diluted in egg water supplemented
857 with 1% DMSO or with Metronidazole (Mtz, 5 mM, Sigma-Aldrich).

858

859 *Live imaging, Sudan black staining of neutrophils, neutrophil ablation and erythrocyte*
860 *determination in zebrafish larvae*

861 At 48 and 72 hpf, larvae were anesthetized in tricaine and mounted in 1%
862 (wt/vol) low-melting-point agarose (Sigma-Aldrich) dissolved in egg water (de Oliveira
863 et al., 2013). Images were captured with an epifluorescence Lumar V12
864 stereomicroscope equipped with green and red fluorescent filters while animals were
865 kept in their agar matrixes at 28.5°C. All images were acquired with the integrated
866 camera on the stereomicroscope and were used for subsequently counting the total
867 number of neutrophils, macrophages or HSPC in whole larvae.

868 In order to decrease pigmentation and improve the signal from Sudan black
869 staining, 24 hpf larvae were incubated in 200 μ M 1-phenyl 2-thiourea (PTU) until 72
870 hpf, when they were anesthetized in buffered tricaine and fixed overnight at 4 °C in 4%
871 methanol-free formaldehyde. On the next day, all the larvae were rinsed with PBS
872 thrice, incubated for 15 min with Sudan black (#380B-1KT, Sigma-Aldrich) and
873 washed extensively in 70% EtOH in water. After that a progressive rehydration was
874 performed: 50% EtOH in PBS and 0.1% Tween 20 (PBT) (Sigma-Aldrich), 25% EtOH
875 in PBT and PBT alone. Finally, the larvae were visualized immediately using a
876 Scope.A1 stereomicroscope equipped with a digital camera (AxioCam ICc 3, Zeiss) (Le
877 Guyader et al., 2008).

878 For neutrophil ablation, larvae *Tg(mpx:Gal4.VP16; UAS:nsfb-mCherry)* were
879 treated at 2 dpf with 5 mM Mtz and kept in dark. At 72 hpf the drug was removed and
880 larvae were treated up to 7 dpf with 1% DMSO alone or containing Ac-YVAD-CMK
881 (100 μ M). The inhibitor was refreshed every 24 h and the larvae were imaged once a
882 day up to 7 dpf and the number of neutrophils determined (Davison et al., 2007;
883 Halpern et al., 2008).

884 Erythrocyte counts were determined by flow cytometry. At 3 dpf, pools of 50
885 *Tg(lcr:eGFP)* larvae were anesthetized in tricaine, minced with a razor blade and
886 incubated at 28°C for 30 min with 0.077 mg/ml Liberase (Roche). Afterwards, 10%
887 FBS was added to inactivate liberase and the resulting cell suspension passed through a
888 40 μ m cell strainer. Flow cytometric acquisitions were performed on a FACSCALIBUR
889 (BD) and analysis was based on forward scatter and side scatter, duplicate exclusion,
890 exclusion of dead cells by addition of SYTOX Blue to a final concentration of 1 μ M,
891 and GFP fluorescence. Before analyzing *Tg(lcr:eGFP)* zebrafish cell suspensions, the
892 flow cytometry gates were set with suspensions from the same number of 3-dpf GFP-
893 negative wild type larvae of the same background. Analyses were performed using
894 FlowJo software (Treestar).

895

896 *Infection assays of zebrafish larvae*

897 For infection experiments, *Salmonella enterica* serovar Typhimurium strain
898 12023 (wild type) provided by Prof. Holden was used. Overnight cultures in Luria-
899 Bertani medium (LB) were diluted 1/5 in LB with 0.3 M NaCl, incubated at 37 °C until
900 1.5 optical density at 600 nm was reached, and finally diluted in sterile PBS. Larvae of
901 2 dpf were anesthetized in embryo medium with 0.16 mg/ml tricaine and 10 bacteria

902 were injected into the yolk sac or otic vesicle. Larvae were allowed to recover in egg
903 water at 28-29 °C, and monitored for clinical signs of disease or mortality over 5 days
904 and neutrophil recruitment up to 24 hpi (Tyrkalska et al., 2016).

905

906 *Whole-mount RNA in situ hybridization (WISH) in zebrafish larvae*

907 Transparent Casper embryos were used for WISH (Thisse et al., 1993). *gata1a*,
908 *spi1b*, *gcsfr*, *cmyb*, *runx1* and *rag1* sense and antisense RNA probes were generated
909 using the DIG RNA Labelling Kit (Roche Applied Science) from linearized plasmids.
910 Embryos were imaged using a Scope.A1 stereomicroscope equipped with a digital
911 camera (AxioCam ICc 3, Zeiss).

912

913 *K562 cell culture and erythroid differentiation assays*

914 K562 cells (CRL-243; American Type Culture Collection) were maintained in
915 RPMI supplemented with 10% FCS, 2 mM Glutamin, and 1% penicillin-streptomycin
916 (Life Technologies). Cells were maintained and split before confluence every 72h. For
917 the differentiation, cells were treated with 50 µM hemin (#16009-13-5, Sigma-Aldrich),
918 prepared as previously described (Smith et al., 2000), in the presence of 0.1% DMSO
919 alone or containing 100 µM Ac-YVAD-CMK or Ac-LEVD-CHO. Cells were collected
920 at different time points (0, 6, 12, 24, 48 hours post-hemin addition), centrifuged, washed
921 with PBS and stored at -80 °C.

922

923 *Caspase-1 activity assay*

924 The caspase-1 activity was determined with the fluorometric substrate Z-
925 YVAD-AFC (caspase-1 substrate VI, Calbiochem) as described previously (Angosto et
926 al., 2012; Lopez-Castejon et al., 2008; Tyrkalska et al., 2016). In brief, 30 pooled
927 zebrafish larvae and 8x10⁵ K562 cells were lysed in hypotonic cell lysis buffer [25 mM
928 4-(2-hydroxyethyl)piperazine-1-ethanesulfonic acid (HEPES), 5 mM ethylene glycol-
929 bis(2-aminoethylether)-N,N,N',N'-tetraacetic acid (EGTA), 5 mM dithiothreitol (DTT),
930 1:20 protease inhibitor cocktail (Sigma-Aldrich), pH 7.5] on ice for 10 min. For each
931 reaction, 80 µg protein were incubated for 90 min at 23° C with 50 µM Z-YVAD-AFC
932 and 50 µl of reaction buffer [0.2% 3-[(3-cholamidopropyl)dimethylammonio]-1-
933 propanesulfonate (CHAPS), 0.2 M HEPES, 20% sucrose, 29 mM DTT, pH 7.5]. After
934 the incubation, the fluorescence of the AFC released from the Z-YVAD-AFC substrate
935 was measured with a FLUOstart spectrofluorometer (BGM, LabTechnologies) at an

936 excitation wavelength of 405 nm and an emission wavelength of 492 nm. One
937 representative caspase-1 activity assay out of the three carried out is shown
938 accompanying each cell count.

939

940 *Laser confocal microscopy*

941 Cells were seeded in Poly-L-Lys Cellware 12mm cover (Corning), 50,000 cells
942 in 100 μ l were allowed to attach to the cover during 10 min at room temperature, then
943 medium and treatment were added. After hemin treatment cells were washed with PBS,
944 fixed with 4% paraformaldehyde in PBS 10 min, incubated 20 min at room temperature
945 with 20 mM glycine, permeabilized with 0.5% NP40 and blocked for 1 h with 2% BSA.
946 Cells were then labeled with corresponding primary antibody, followed by Alexa 568-
947 conjugated secondary antibody (Thermo Fisher Scientific). Samples were mounted
948 using a mounting medium from Dako and examined with a Leica laser scanning
949 confocal microscope AOBS and software (Leica Microsystems). The images were
950 acquired in a 1,024 \times 1,024 pixel format in sequential scan mode between frames to
951 avoid cross-talk. The objective used was HCX PL APO CS \times 63 and the pinhole value
952 was 1, corresponding to 114.73 μ m.

953

954 *Immunoblotting*

955 Lysis buffer for mammalian cell lysis contained 50 mM Tris-HCl (pH 7.5), 150
956 mM NaCl, 1 mM EDTA, 1 mM EGTA, 1% (w/v) NP-40 and fresh protease inhibitor
957 (1/20, P8340, Sigma-Aldrich), while for zebrafish larvae lysis contained 1% SDS.
958 Protein quantification was done with BCA kit using BSA as a standard. Cell lysates (40
959 μ g) in SDS sample buffer were subjected to electrophoresis on a polyacrylamide gel and
960 transferred to PVDF membranes. The membranes were incubated for 1 h with TTBS
961 containing 5% (w/v) skimmed dried milk powder or 2% (w/v) BSA. The membranes
962 were immunoblotted in the same buffer 16 h at 4°C with the indicated primary
963 antibodies. The blots were then washed with TTBS and incubated for 1 h at room
964 temperature with secondary HRP-conjugated antibodies diluted 2,500-fold in 5% (w/v)
965 skimmed milk in TTBS. After repeated washes, the signal was detected with the
966 enhanced chemiluminescence reagent and ChemiDoc XRS Biorad. The primary
967 antibodies used are: rabbit polyclonal to human GATA1 (1/200, #sc1234, Santa Cruz
968 Biotechnology) for confocal assay, rabbit mAb to human GATA1 (1/200, #3535, Cell
969 Signaling) for immunoblotting, rabbit polyclonal to CASP1 (1/200, #sc56036 Santa

970 Cruz Biotechnology) for confocal assay, rabbit polyclonal to zebrafish Gata1a and
971 Spi1b (1/2000, #GTX128333 and GTX128266, GeneTex), rabbit polyclonal to histone
972 H3 (1/200, #ab1791, Abcam) and Monoclonal ANTI-FLAG® M2-Peroxidase (HRP)
973 antibody produced in mouse (A8592 Sigma-Aldrich). Densitometry analysis has been
974 performed using Fiji Image J software (Schindelin et al., 2012).

975

976 *Immunoprecipitation and recombinant caspase-1 assay*

977 Pull down assays were also performed as described previously (Tyrkalska et al.,
978 2017), with small modifications. Cells were washed twice with PBS, solubilized in lysis
979 buffer (50 mM Tris-HCl, , pH 7.7, 150 mM NaCl, 1% NP-40 and protease inhibitor
980 cocktail) during 30 min in agitation and centrifuged ($13,000 \times g$, 10 min). Cell lysate (1
981 mg) was incubated for 2 h at 4°C under gentle agitation with 40 µl of slurry of
982 ANTIFLAG® M2 (#A2220 Sigma-Aldrich). The immunoprecipitates were washed four
983 times with lysis buffer containing 0.15 M NaCl, washed twice with PBS and incubated
984 with 10 IU recombinant caspase-1 (#GTX65025, GeneTex) in reaction buffer (50 mM
985 HEPES, pH 7.2, 50mM NaCl, 0.1% Chaps, 10 mM EDTA, 5% Glycerol, and 10 mM
986 DTT) during 2 h at 37 °C. The resin was boiled in SDS sample buffer 5 min at 95 °C
987 and the bound proteins were resolved on 4-15% SDS-PAGE (BioRad TGX #456-1084)
988 and transferred to PVDF membranes for 1h at 300 mA. Blots were probed with
989 antibodies to FLAG and GATA1 (see above).

990

991 *Analysis of gene expression*

992 Total RNA was extracted from 10^6 K562 cells, whole embryos or larvae (60) or
993 larval tails (100) with TRIzol reagent (Thermo Fisher Scientific) following the
994 manufacturer's instructions and treated with DNase I, amplification grade (1 U/µg
995 RNA; Invitrogen). SuperScript III RNase H⁻ Reverse Transcriptase (Invitrogen) was
996 used to synthesize first-strand cDNA with oligo(dT)18 primer from 1 µg of total RNA
997 at 50°C for 50 min. Real-time PCR was performed with an ABI PRISM 7500
998 instrument (Applied Biosystems) using Power SYBR Green Master Mix (ThermoFisher
999 Scientific). Reaction mixtures were incubated for 10 min at 95°C, followed by 40 cycles
1000 of 15 s at 95°C, 1 min at 60°C, and finally 15 s at 95°C, 1 min 60°C and 15 s at 95°C.
1001 For each mRNA, gene expression was normalized to the ribosomal protein S11 (*rps11*)
1002 for zebrafish or β-actin (*ACTB*) for human cells content in each sample following the

1003 Pfaffl method (Pfaffl, 2001). The primers used are shown in (Table S2). In all cases,
1004 each PCR was performed with triplicate samples and repeated with at least two
1005 independent samples.

1006

1007 *Isolation of mouse HSCs*

1008 Male Spi1-eYFP and Gata1-mCherry mice were euthanized and isolation of
1009 HSCs was performed according to previously described protocols (Cabezas-Wallscheid
1010 et al., 2014; Hoppe et al., 2016; Kiel et al., 2005). Briefly, femurs, tibiae and vertebrae
1011 of adult mice were isolated and crushed in FACS buffer (2% FCS (PAA) + 1mM EDTA
1012 in PBS). Bone marrow suspension was subjected to ACK (Lonza) lysis buffer for 2
1013 minutes followed by lineage depletion steps including incubation with biotinylated
1014 antibodies cocktail of CD3e, CD19, B220, CD11b, Gr-1 and Ter-119 for 7 minutes,
1015 streptavidin-conjugated beads (Roche) for 7 minutes and immune-magnetic (Stem Cell
1016 Technologies) separation for 7 minutes. Lineage depleted cells were stained with color-
1017 conjugated primary antibodies for 90 minutes. FACS sorting of HSCs was performed
1018 on FACS ARIA III (BD Biosciences) using the Lineage⁻ Sca1⁺ cKit⁺ CD34⁻ CD48⁻
1019 CD135⁻ CD150⁺. All steps were performed at 4°C.

1020

1021 *Mouse single-cell liquid culture colony assay*

1022 Single-cell sort of HSCs was performed in plastic-bottom 384 well plates
1023 (Greiner Bio-one) using FACS ARIA III under standard permissive culture media as
1024 described (IMDM (Gibco) + 5 % BIT (Stem Cell Technologies) + P/S (Gibco) + SCF
1025 + Epo + Tpo + IL3 + IL6) with or without 100 μM Ac-YVAD-CMK. Plates were
1026 incubated at 37° C and 5% CO₂. At day 8, color-conjugated antibodies against lineage
1027 markers (CD41-APC + CD16/32-BV421) were added (1:5000 dilution) in wells,
1028 incubated for 3 hours at 37°C and 5% CO₂ and imaging of hematopoietic colonies was
1029 performed on Nikon Eclipse Ti-E microscope. Colonies were scored manually.
1030 Granulocyte-monocyte colonies were indicated by morphology, CD16/32 and SPI-
1031 eYFP expression while megakaryocyte-erythrocyte colonies were indicated by
1032 morphology, CD41 and GATA1-mCherry expression as previously described (Hoppe et
1033 al., 2016).

1034

1035

1036

1037 *Time-lapse imaging of mouse HSCs*

1038 HSCs were sorted using FACS ARIA III and seeded in plastic-bottom 384 well
1039 plates (Greiner Bio-one) in multi-lineage supporting culture media as described (Hoppe
1040 et al., 2016) (IMDM (Gibco) + 5 % BIT (Stem Cell Technologies) + P/S (Gibco) + SCF
1041 + Epo + Tpo + IL3 + IL6) with or without 100 μ M Ac-YVAD-CMK. Time-lapse
1042 imaging and quantification of SPI1-eYFP and GATA1-mCherry in HSCs was
1043 performed using previously established protocols (Etzrodt et al., 2018; Hilsenbeck et al.,
1044 2017; Hilsenbeck et al., 2016; Hoppe et al., 2016).

1045

1046 *Quantification and Statistical Analysis*

1047 Data are shown as mean \pm SEM and were analyzed by analysis of variance
1048 (ANOVA) and a Tukey or Bonferroni multiple range test to determine differences
1049 among groups. The differences between two samples were analyzed by the Student *t*-
1050 test. Fisher's exact and Chi-square tests were used for the analysis of contingency
1051 tables. A log rank test with the Bonferroni correction for multiple comparisons was used
1052 to calculate the statistical differences in the survival of the different experimental
1053 groups.

KEY RESOURCES TABLE

REAGENT or RESOURCE	SOURCE	IDENTIFIER
Antibodies		
Rabbit polyclonal to human GATA1	Santa Cruz Biotechnology	Cat#sc1234
Rabbit mAb to human GATA1	Cell Signaling	Cat#3535
Rabbit polyclonal to CASP1	Santa Cruz Biotechnology	Cat#sc56036
Rabbit polyclonal to zebrafish Gata1a	GeneTex	Cat#GTX128333
Rabbit polyclonal to zebrafish Spi1b	GeneTex	Car#GTX128266
Rabbit polyclonal to histone H3	Abcam	Cat#ab1791
Monoclonal ANTI-FLAG® M2-Peroxidase (HRP) antibody produced in mouse	Sigma-Aldrich	Cat#A8592
Streptavidin-BV711	BD Biosciences	Cat#563262
anti-Sca1 conjugated with BV510	Biolegend	Cat#108129
anti-cKIT conjugated with BV421	Biolegend	Cat#105828
anti-CD135 conjugated with PerCPeFL710	eBioscience	Cat#46-1351-82
anti-CD34 conjugated with eFL660	eBioscience	Cat#50-0341-82
anti-CD48 conjugated with APCeFL780	eBioscience	Cat#47-0481-82
anti-CD150 conjugated with BV650	Biolegend	Cat#115932
anti-B220-Biotin	eBioscience	Cat#13-0452-86
anti-CD19-biotin	eBioscience	Cat#13-0191-86
antiCd3e-biotin	eBioscience	Cat#13-0031-85
anti-CD11b-biotin	eBioscience	Cat#13-0112-85
anti-Gr1-biotin	eBioscience	Cat#13-5931-85
anti-Ter119-biotin	eBioscience	Cat#13-5921-85
anti-CD41-APC	eBioscience	Cat#17-0411-82
anti-CD16/32-BV421	Biolegend	Cat#101332
Bacterial and Virus Strains		
<i>Salmonella enterica</i> serovar Typhimurium, strain 12023 (wild type)	Prof. David Holden	
Chemicals, Peptides, and Recombinant Proteins		
EnGen® Cas9 NLS from <i>Streptococcus pyogenes</i>	New England Biolabs	Cat#M0646

Ac-YVAD-CMK	Peptanova	Cat#3180-v
Ac-YVAD-CHO	Peptanova	Cat#3165-v
Ac-LEVD-CHO	Peptanova	Cat#864-42-v
Metronidazole	Sigma Aldrich	Cat#M1547
Sudan black	Sigma-Aldrich	Cat#380B-1KT
Z-YVAD-AFC	Merck	Cat#688225
ANTIFLAG® M2	Sigma-Aldrich	Cat#A2220
Recombinant caspase-1	GeneTex	Cat#GTX65025
4-15% SDS-PAGE	BioRad	Cat#456-1084
DNase I, amplification grade	ThermoFisher Scientific	Cat#18068015
SuperScript III RNase H ⁻ Reverse Transcriptase	ThermoFisher Scientific	Cat#18080085
Power SYBR Green Master Mix	ThermoFisher Scientific	Cat#4368708
Liberase TM research Grade	Sigma-Aldrich	Cat#05401119001
Experimental Models: Cell Lines		
K562	ATCC	Cat#CCL243
Experimental Models: Organisms/Strains		
Zebrafish casper line (<i>roy^{a9/a9}; nacre^{w2/w2}</i>)	Prof. LI Zon	
<i>Tg(mpx:eGFP)ⁱ¹¹⁴</i>	Prof. SA Renshaw	
<i>Tg(mpeg1:eGFP)^{g122}</i>	Prof. G Lieschke	
<i>Tg(mpeg1:GAL4)^{g125}</i>	Prof. G Lieschke	
<i>Tg(lyz:dsRED)^{nz50}</i>	Prof. P Crosier	
<i>Tg(mpx:Gal4.VP16)ⁱ²²²</i>	Prof. SA Renshaw	
<i>Tg(lcr:eGFP)^{cz3325}</i>	Prof. LI Zon	
<i>Tg(runx1:GAL4)^{utn6}</i>	Prof. LI Zon	
<i>Tg(UAS:nfsB-mCherry)^{c264}</i>	Prof. M. Halpern	
<i>Tg(spint1a)^{hi2217}</i>	Prof. M. Hammerschmidt	
SPI1-eYFP/GATA1-mCherry1 reporter mice (C57BL/6J background)	Prof. Timm Schroeder	
Recombinant DNA		
Tol2kit	Dr. K. Kwan	http://tol2kit.genetics.utah.edu/index.php/Main_Page

Figure 1

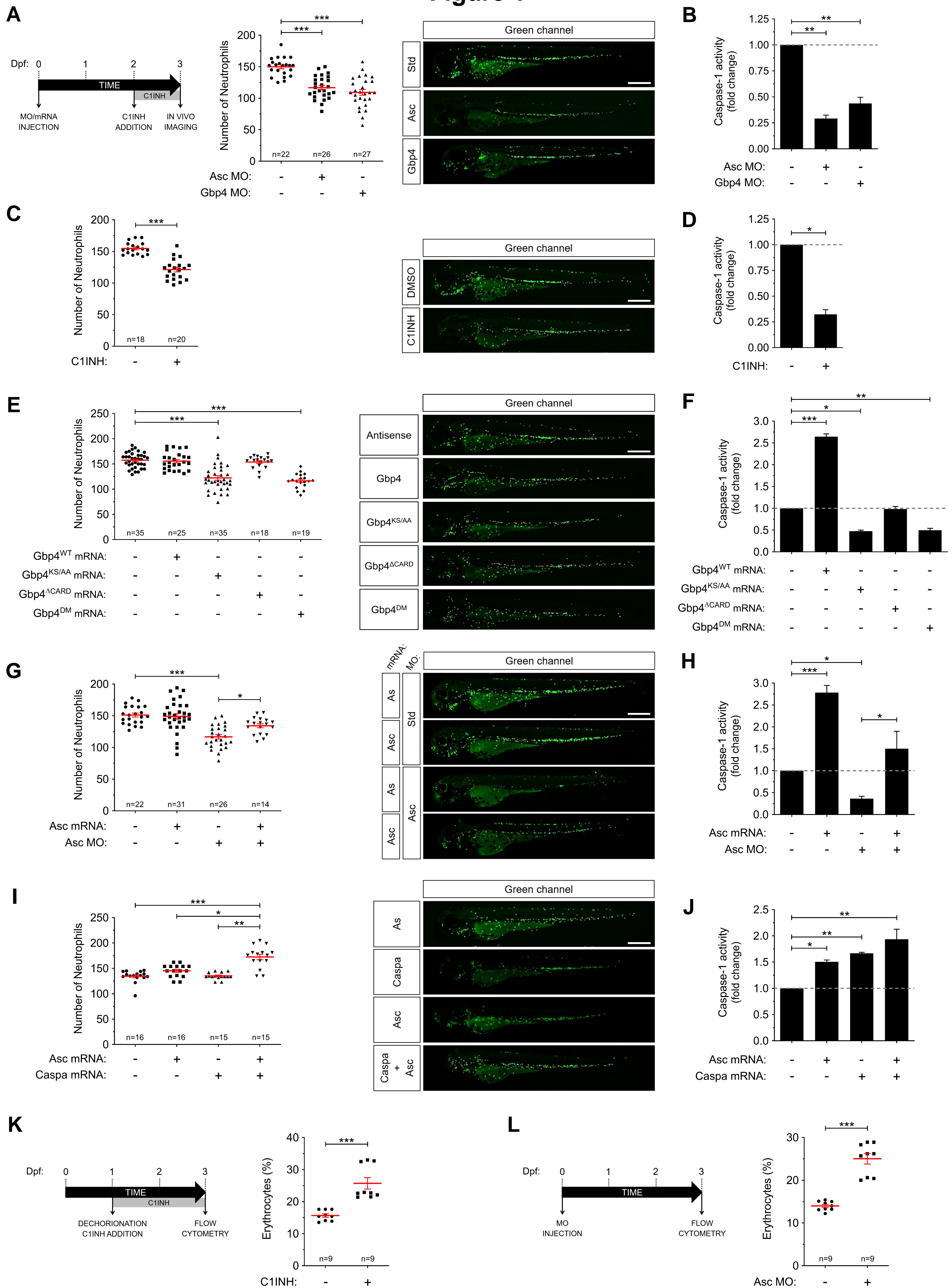


Figure 2

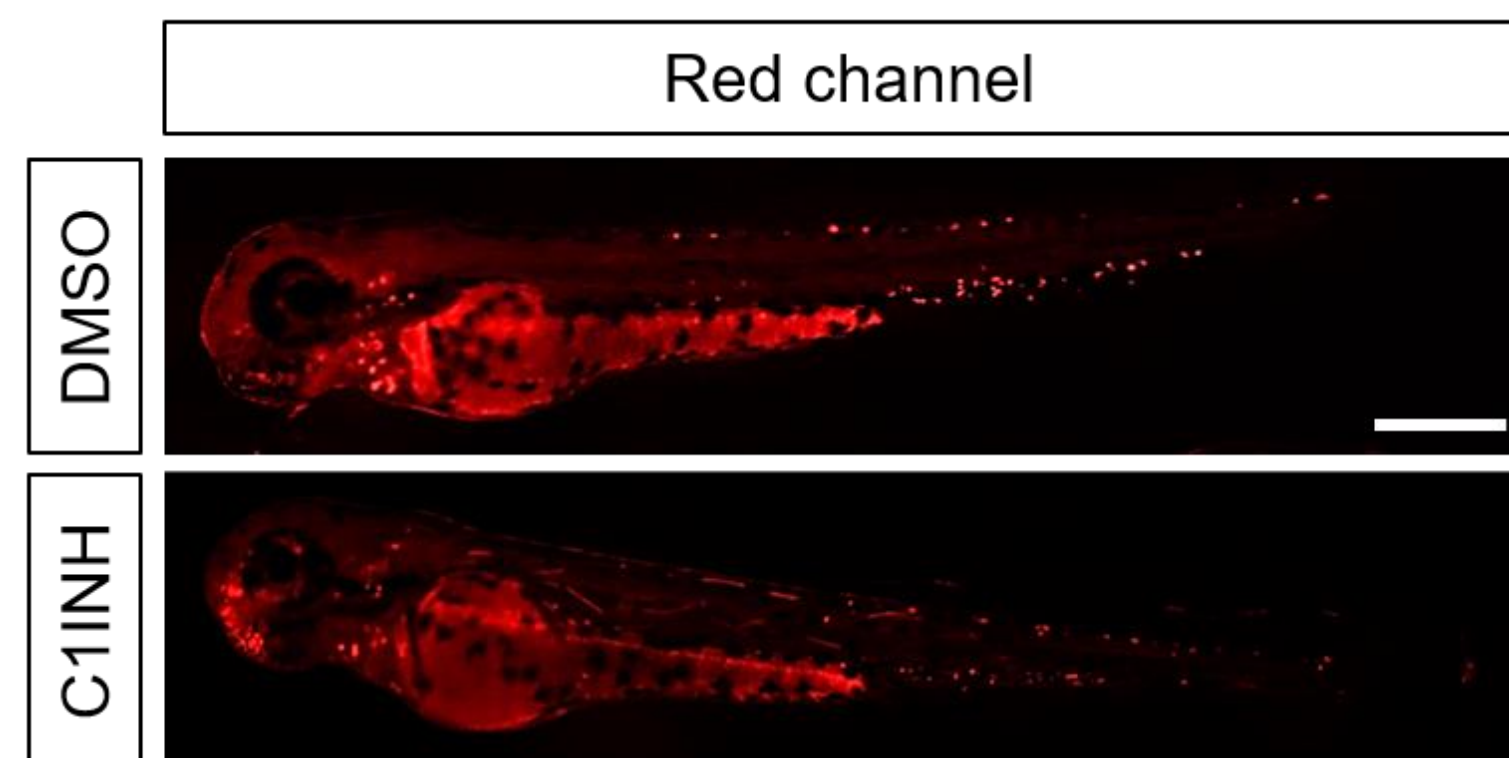
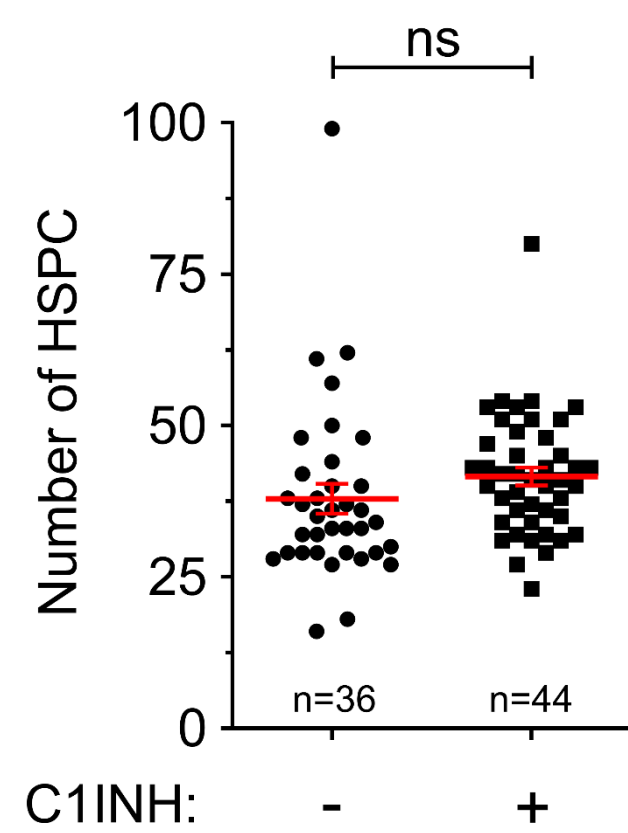
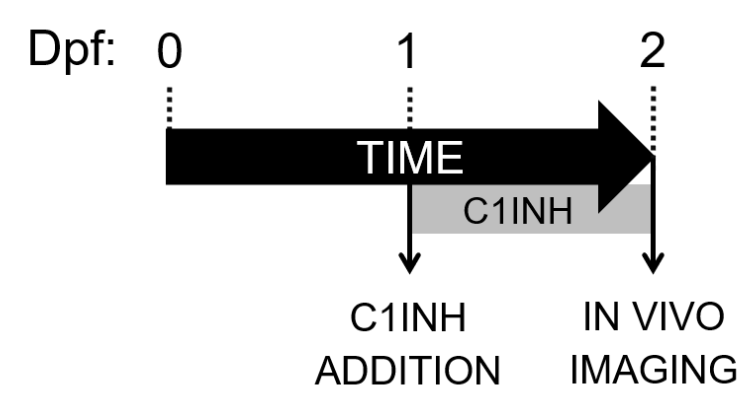
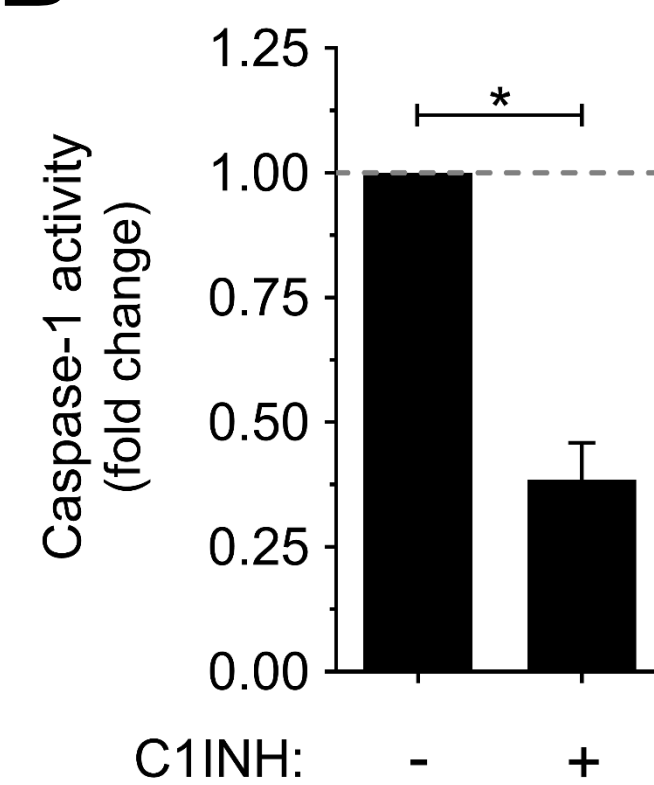
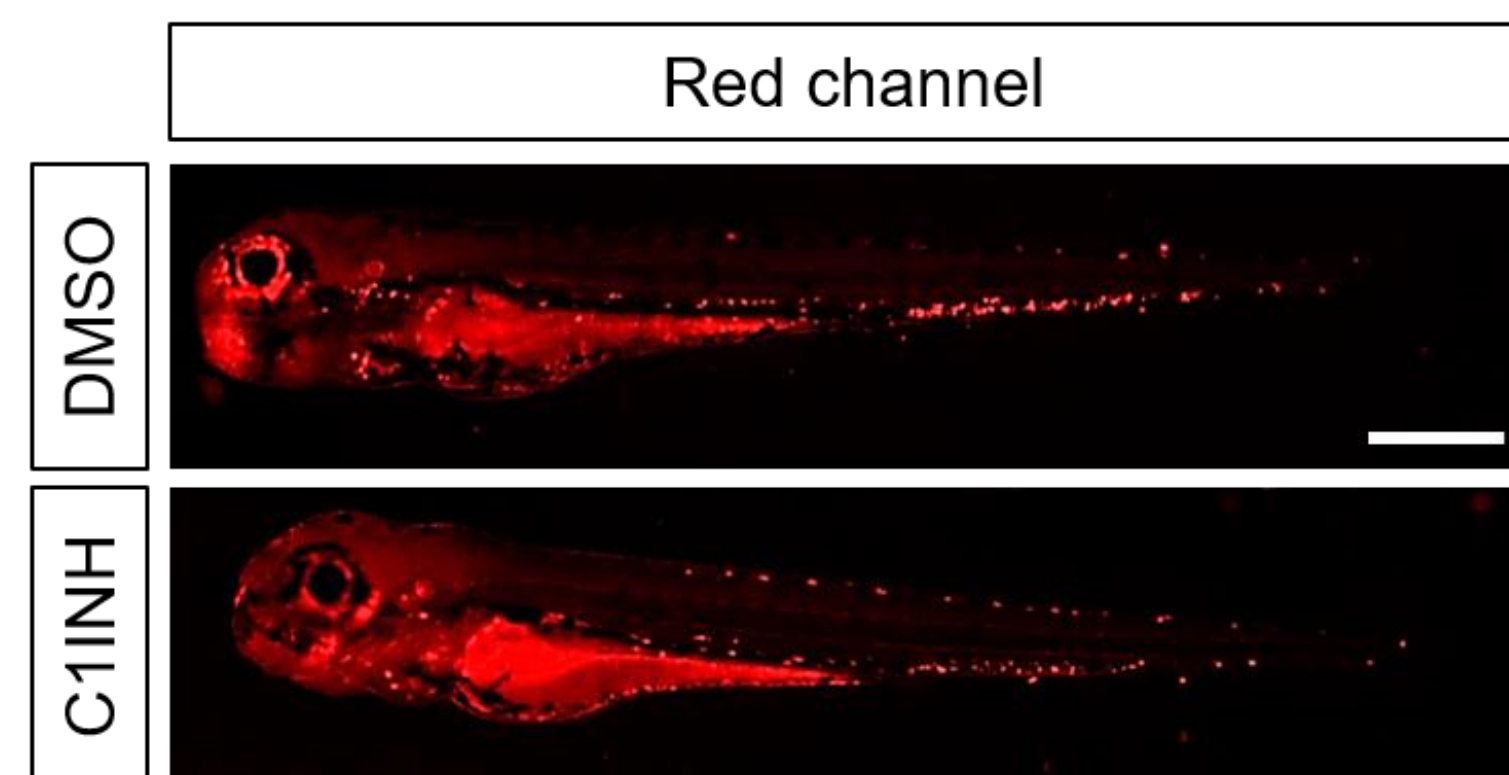
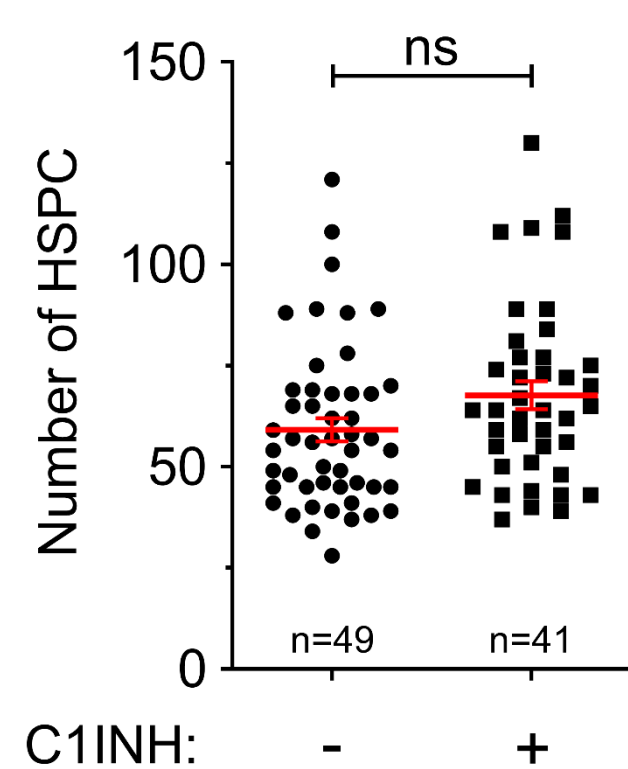
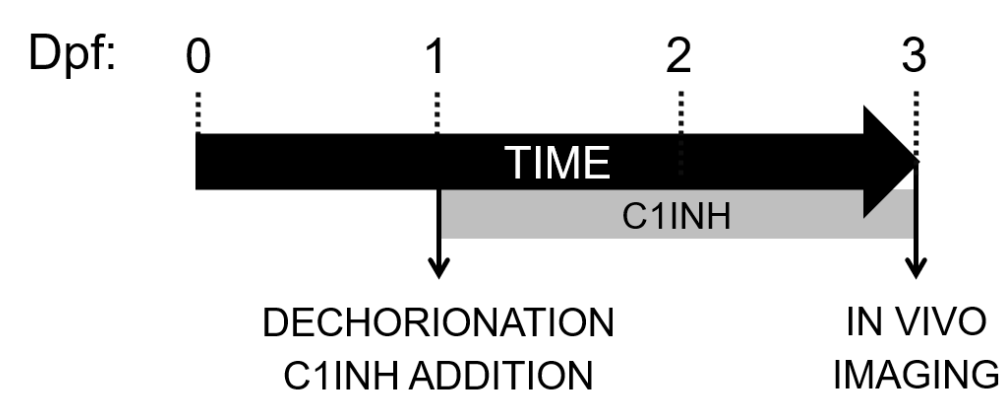
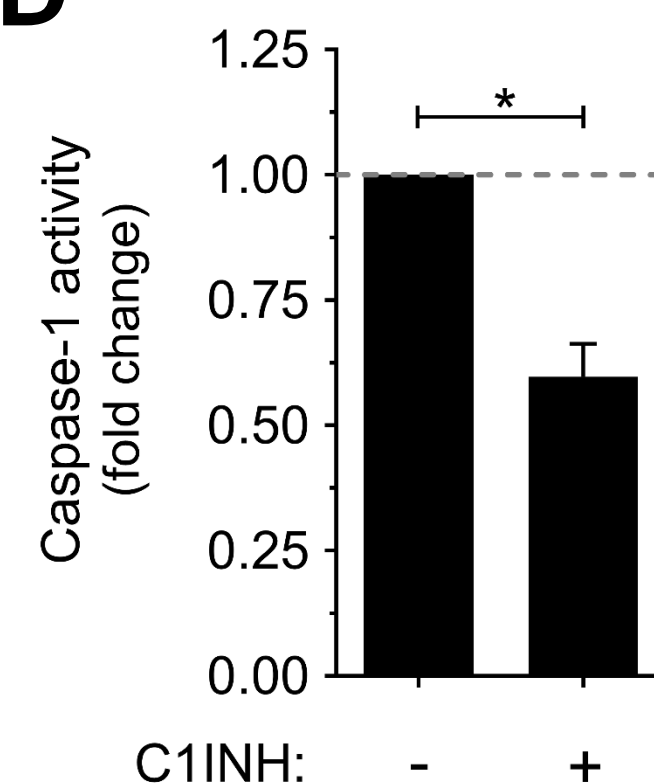
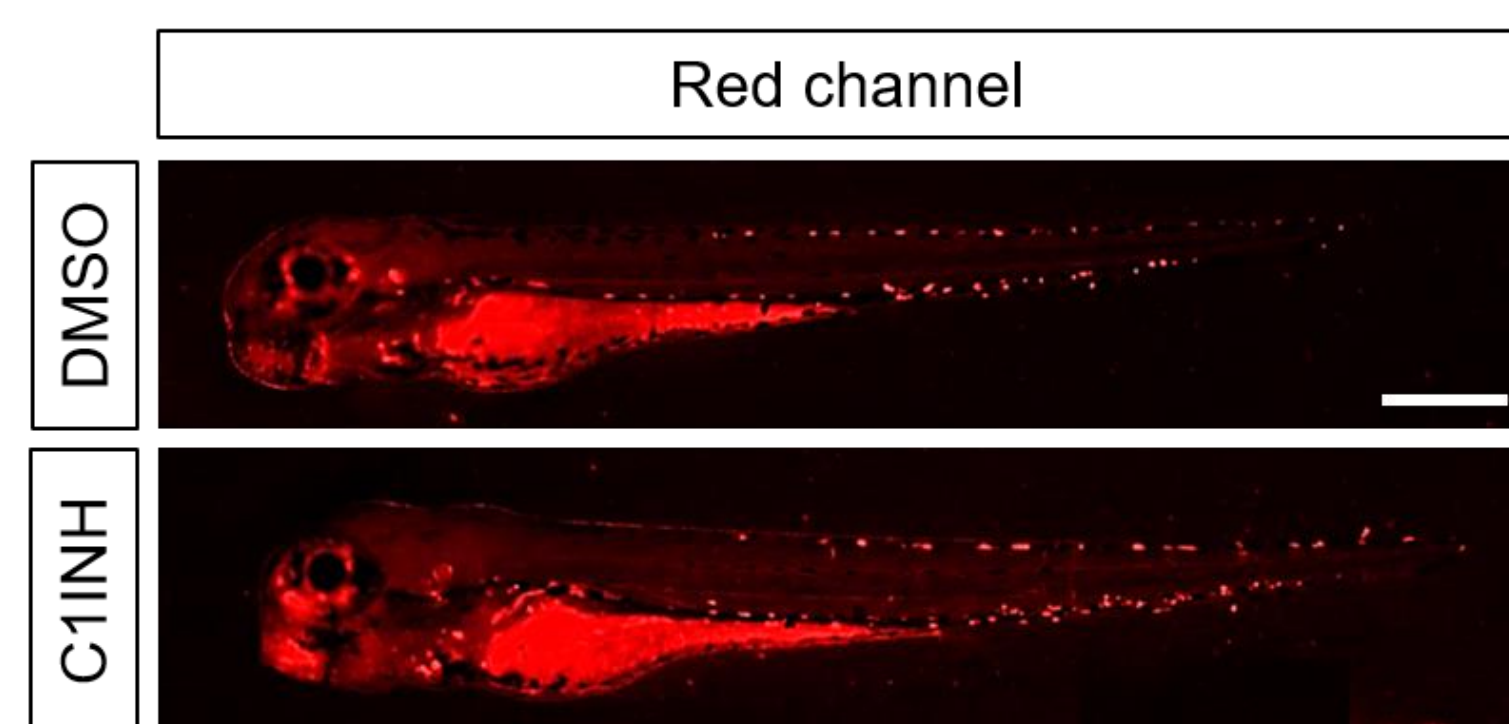
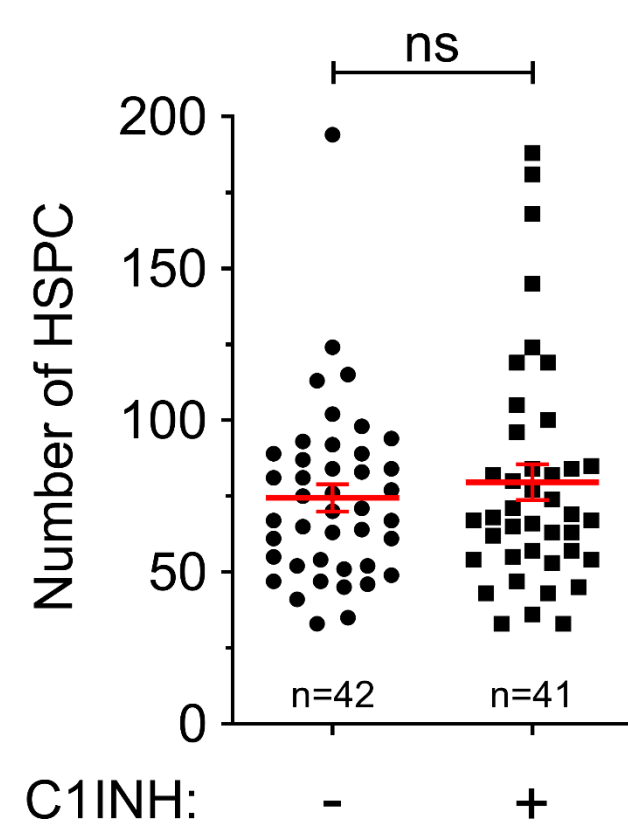
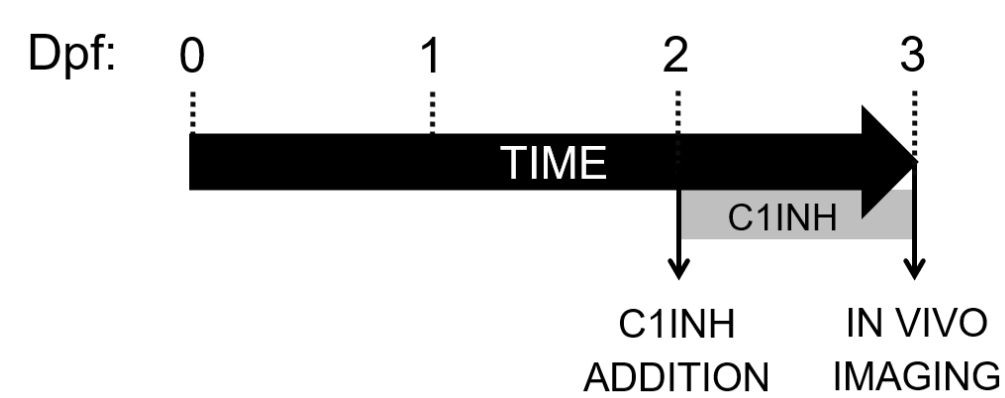
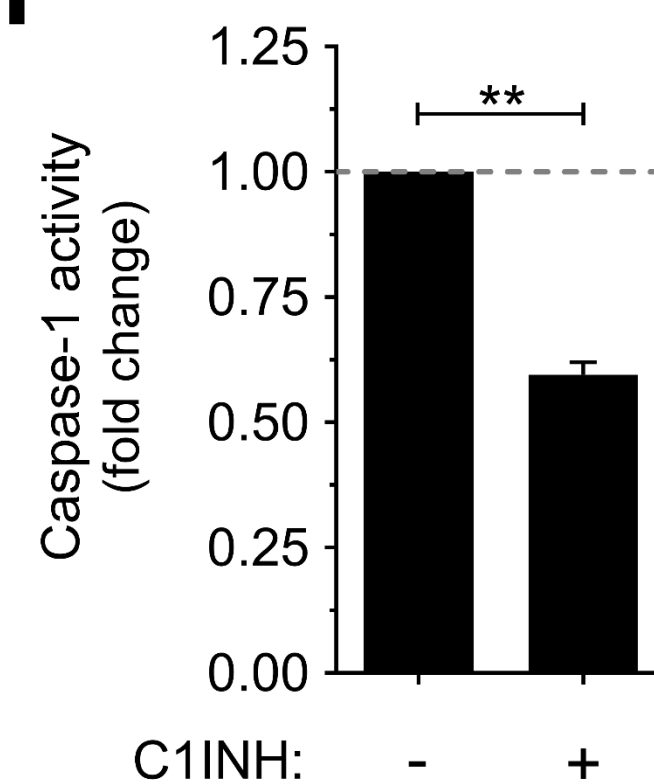
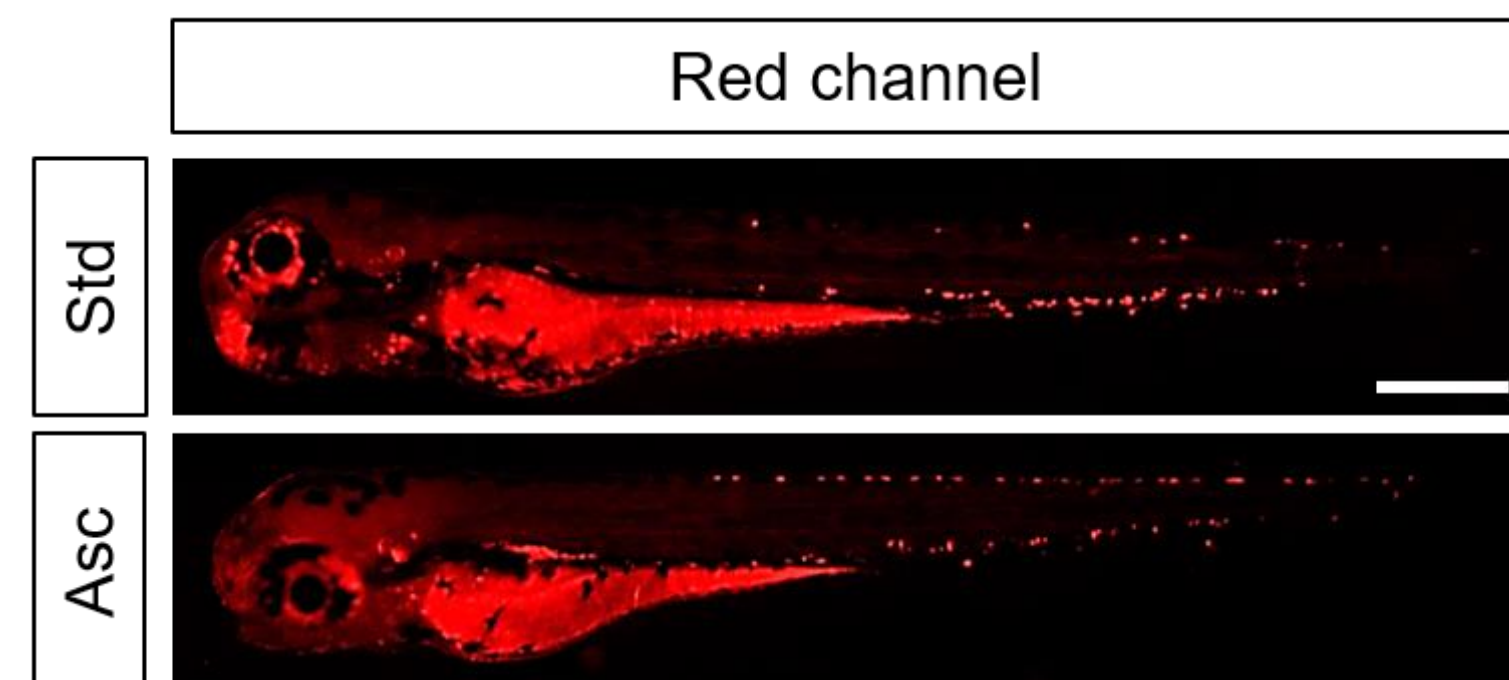
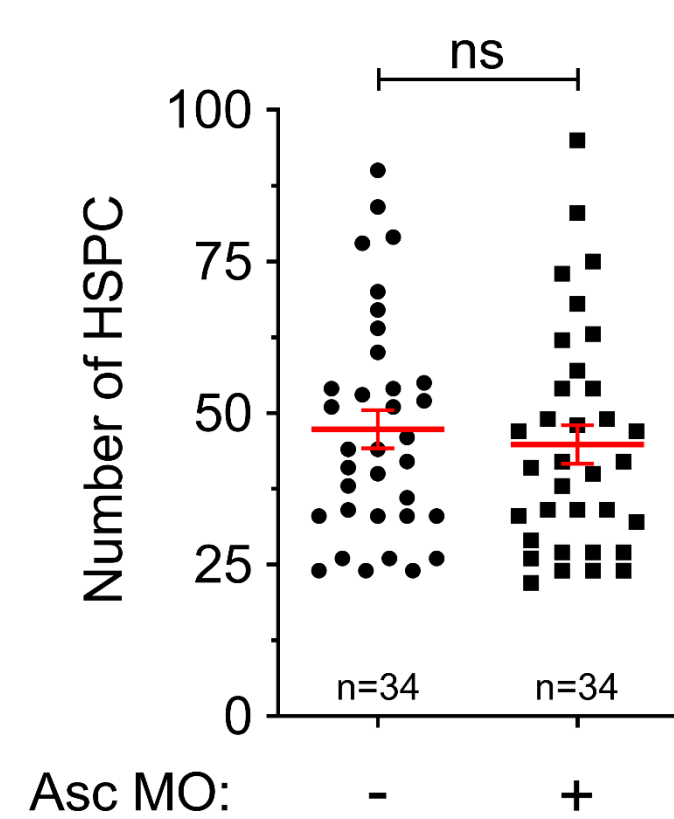
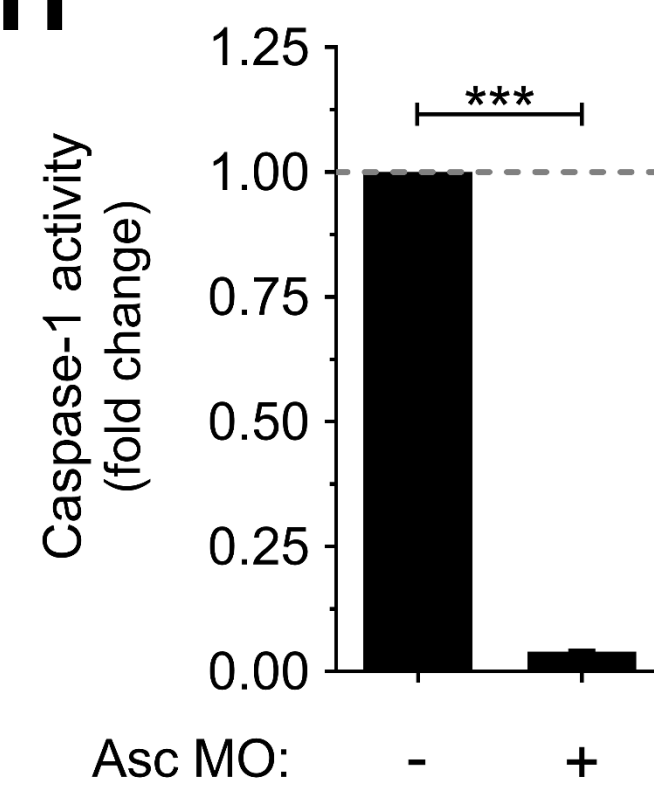
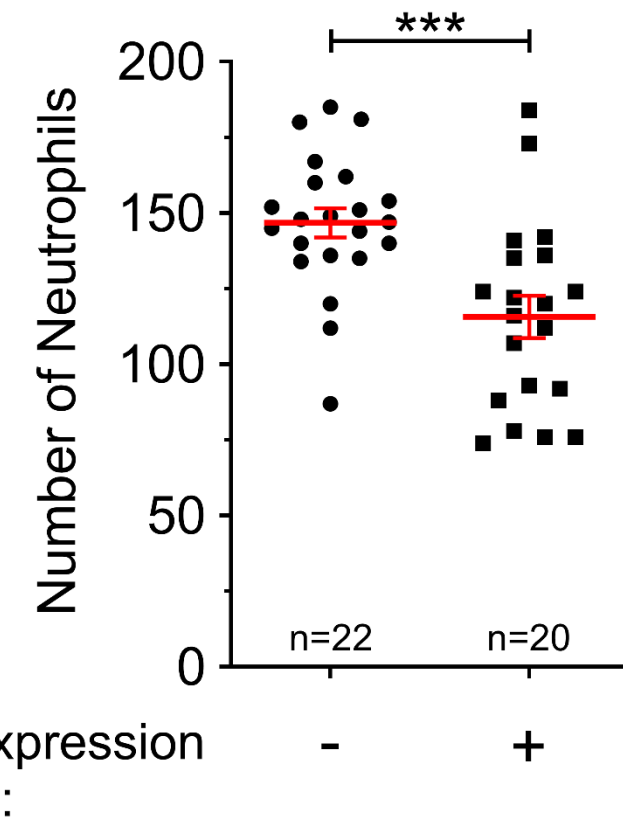
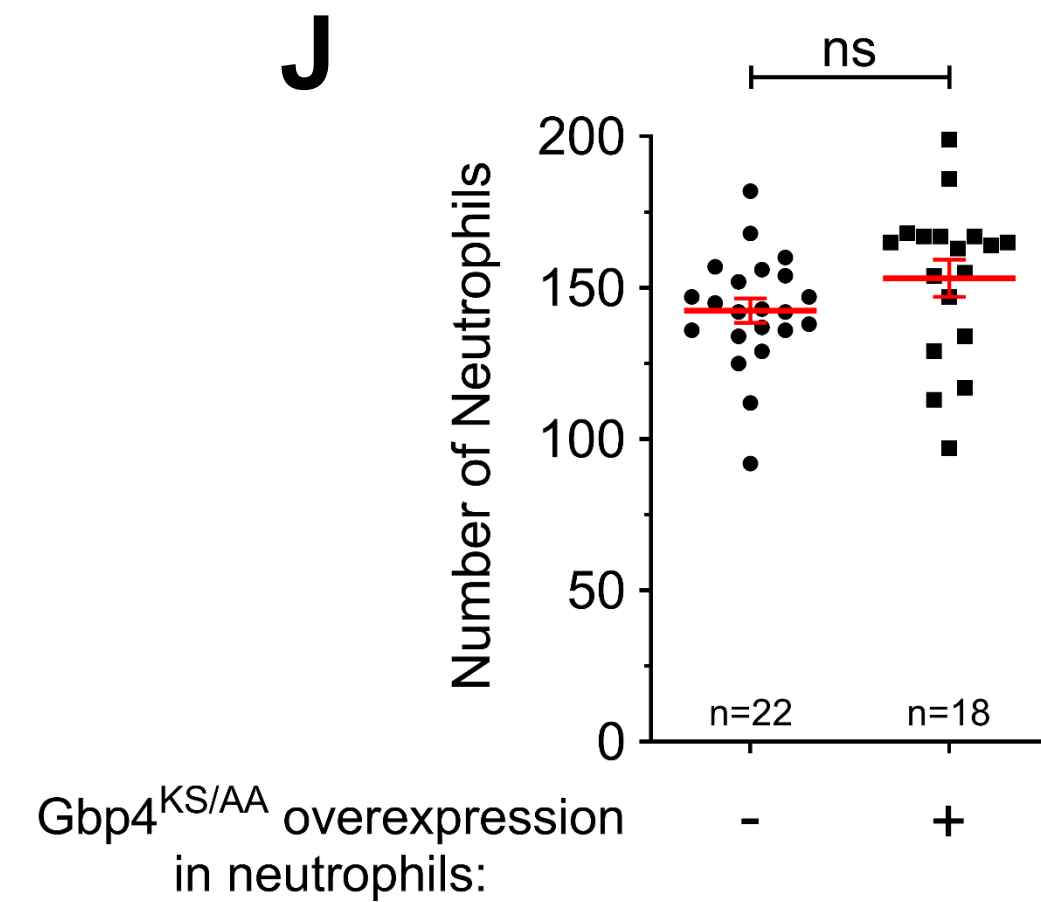
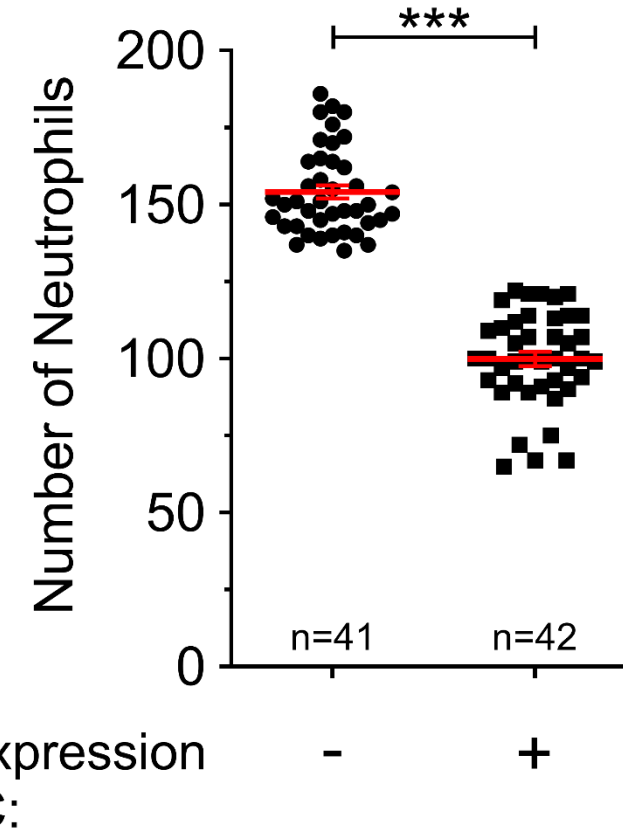
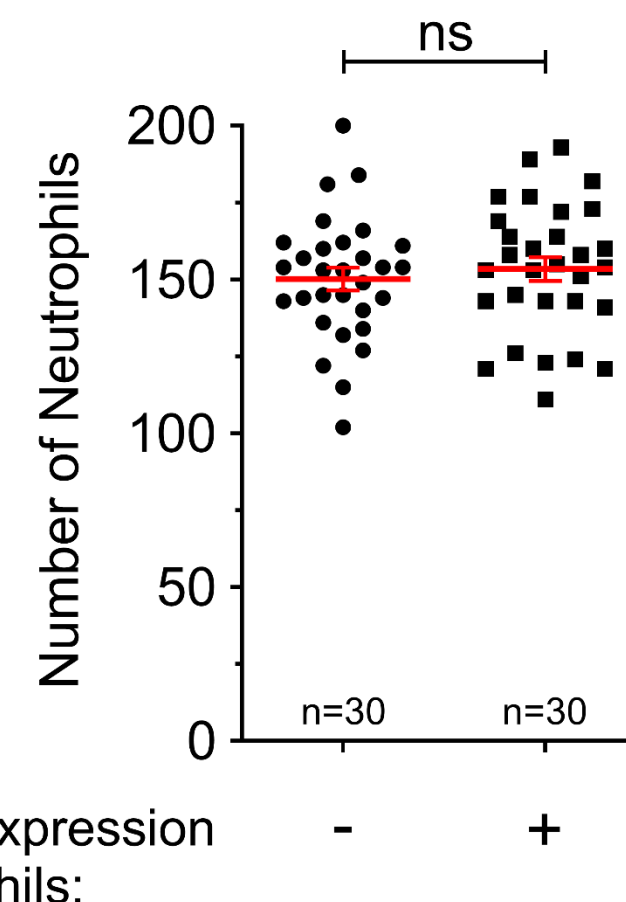
A**B****C****D****E****F****G****H****I****J****K****L**

Figure 4

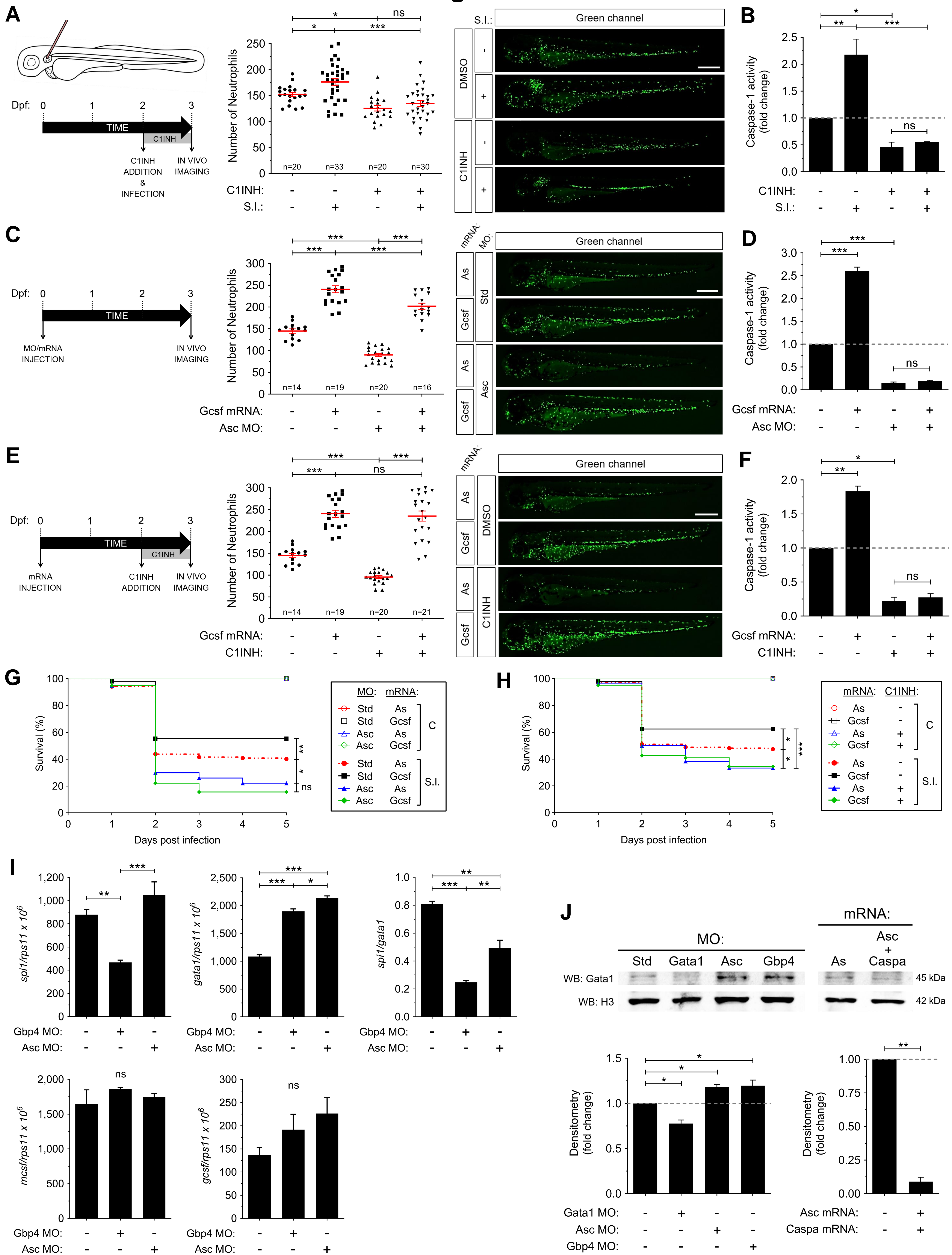


Figure 5

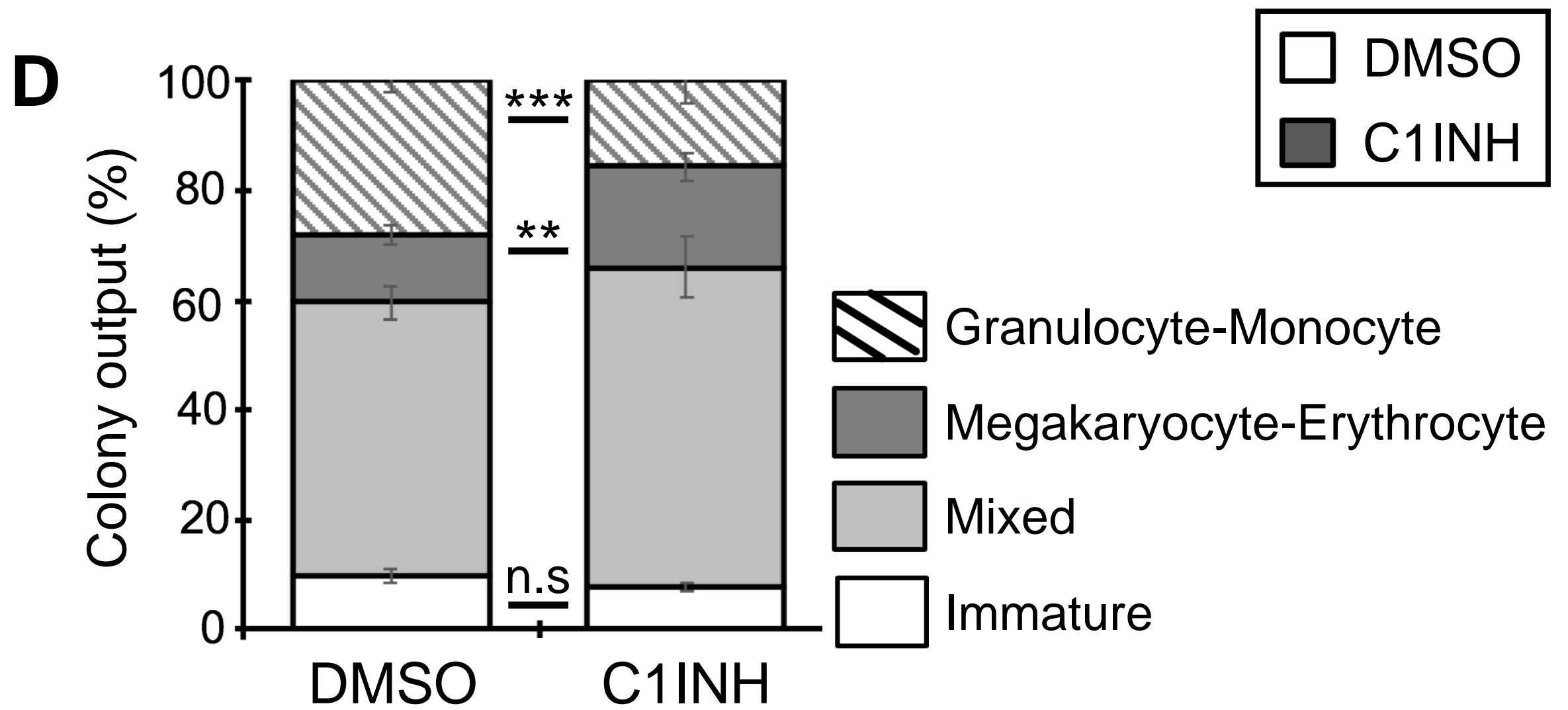
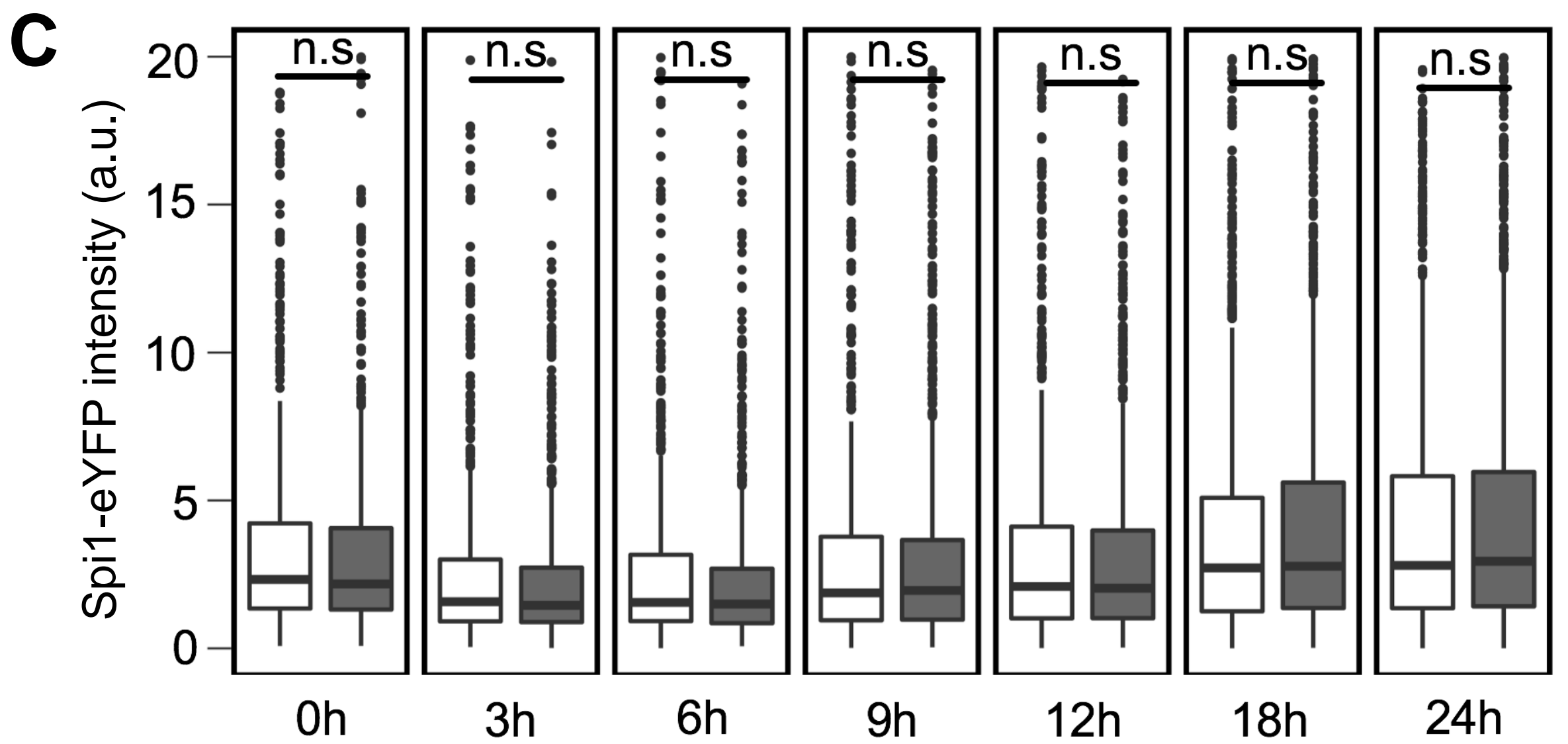
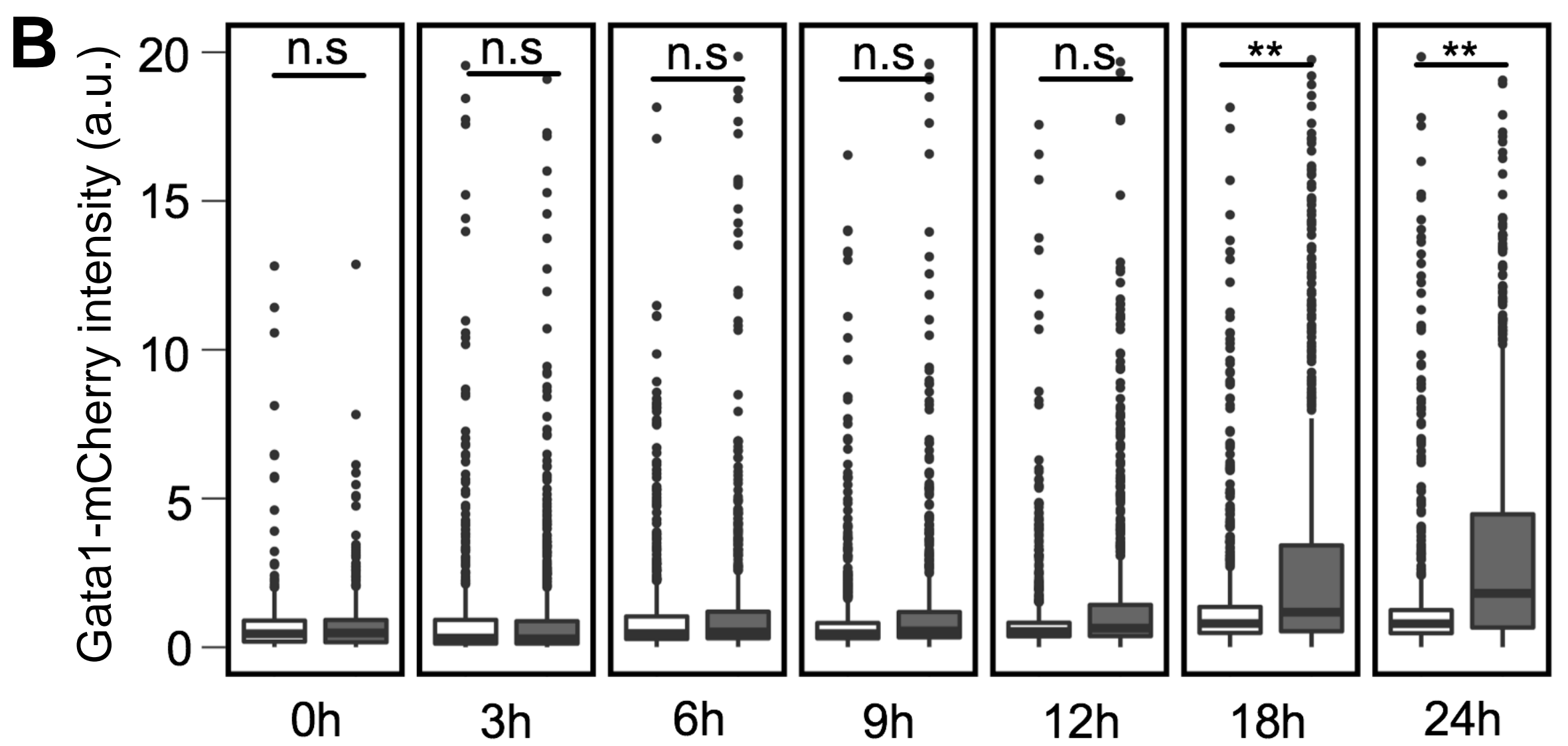
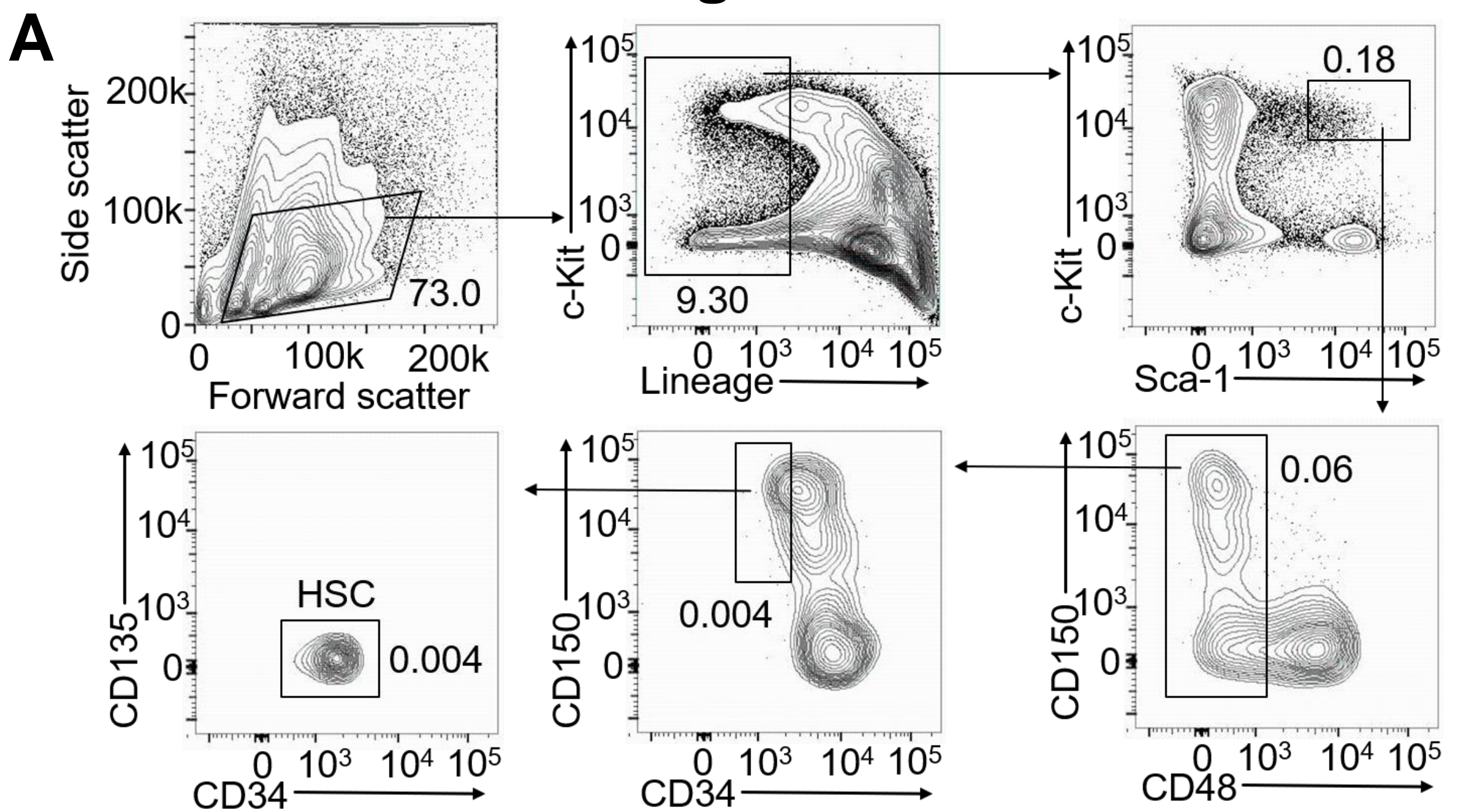


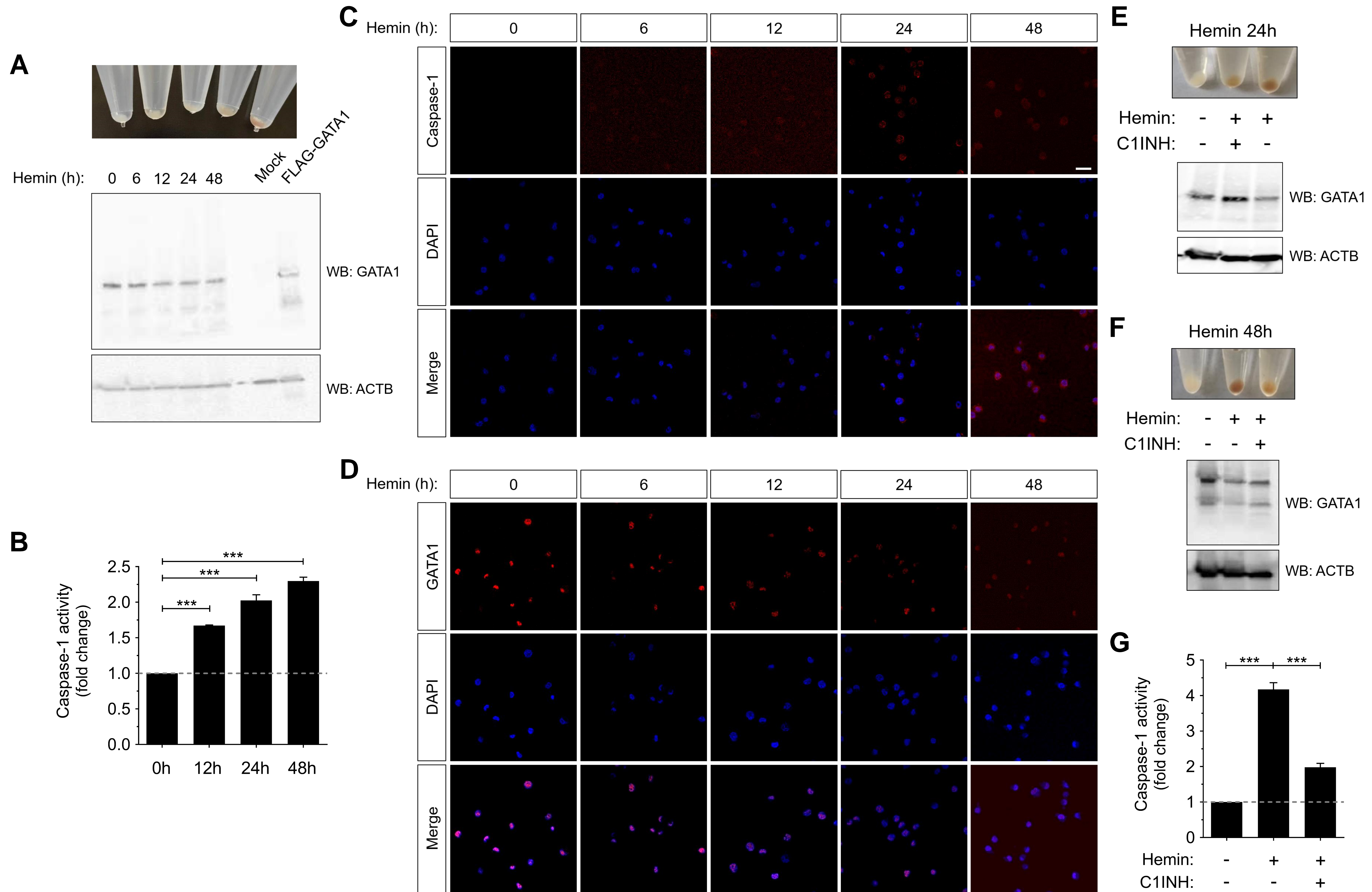
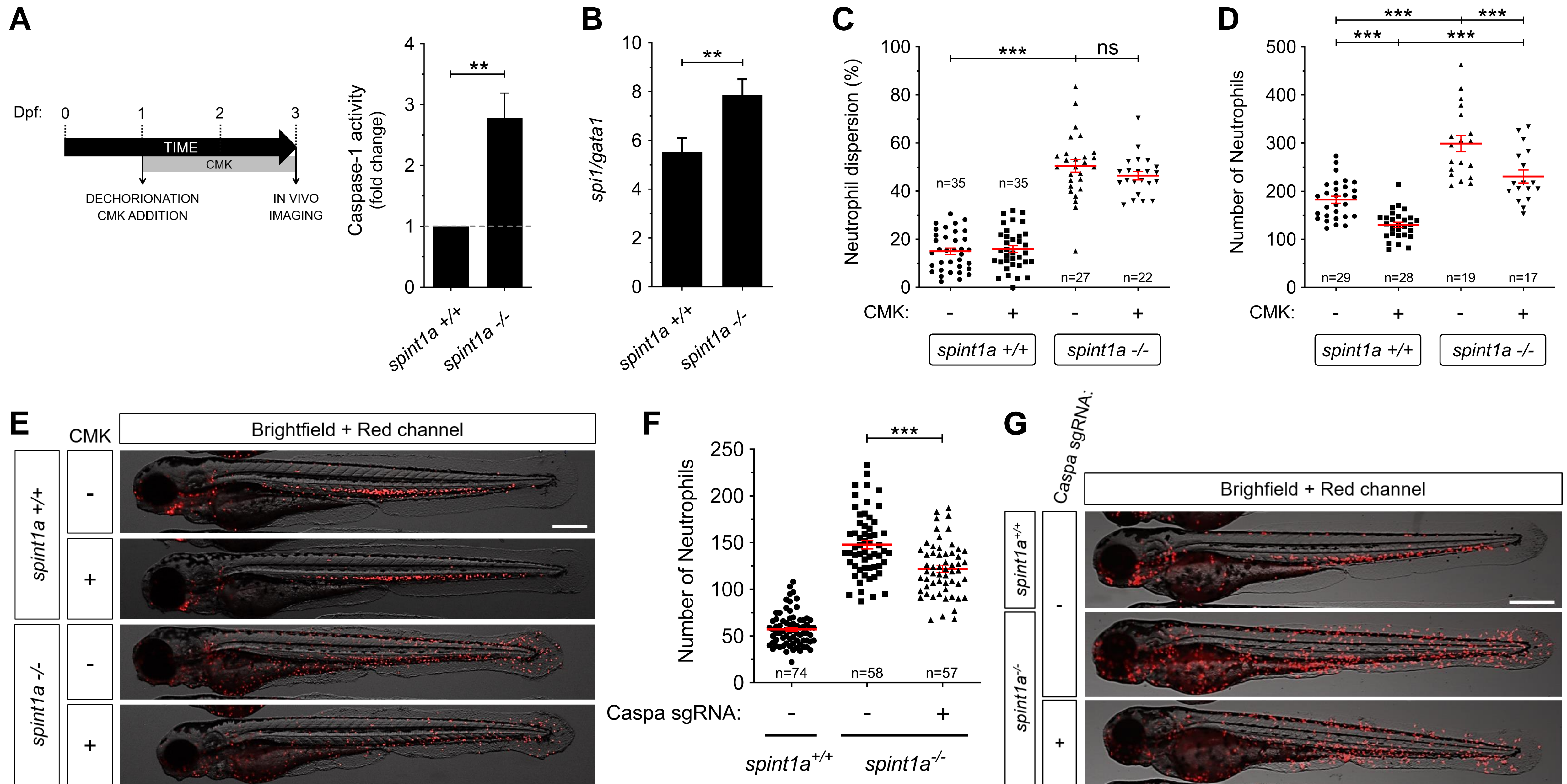
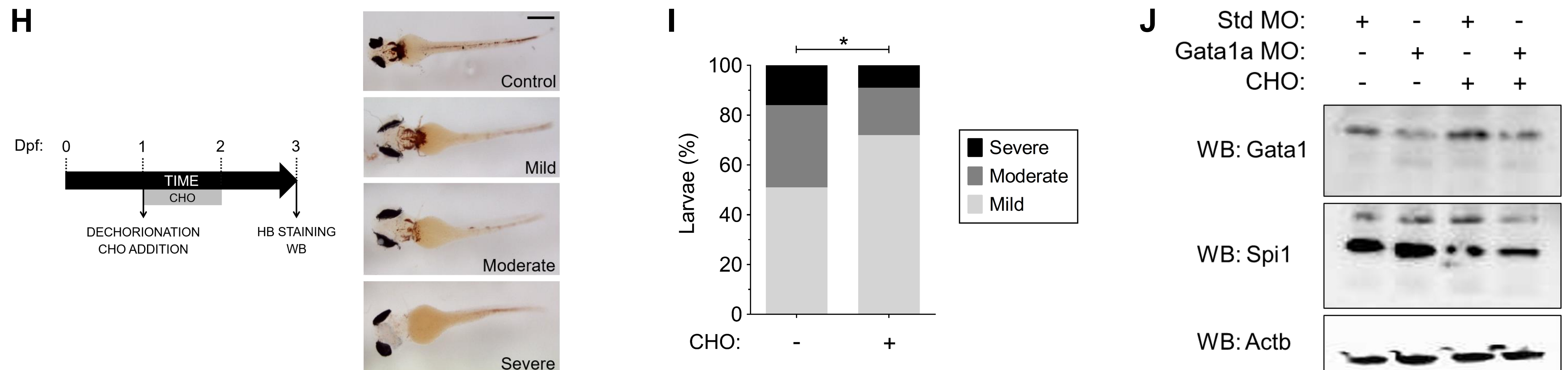
Figure 6

Figure 7

Neutrophilic inflammation



Diamond-Blackfan anemia



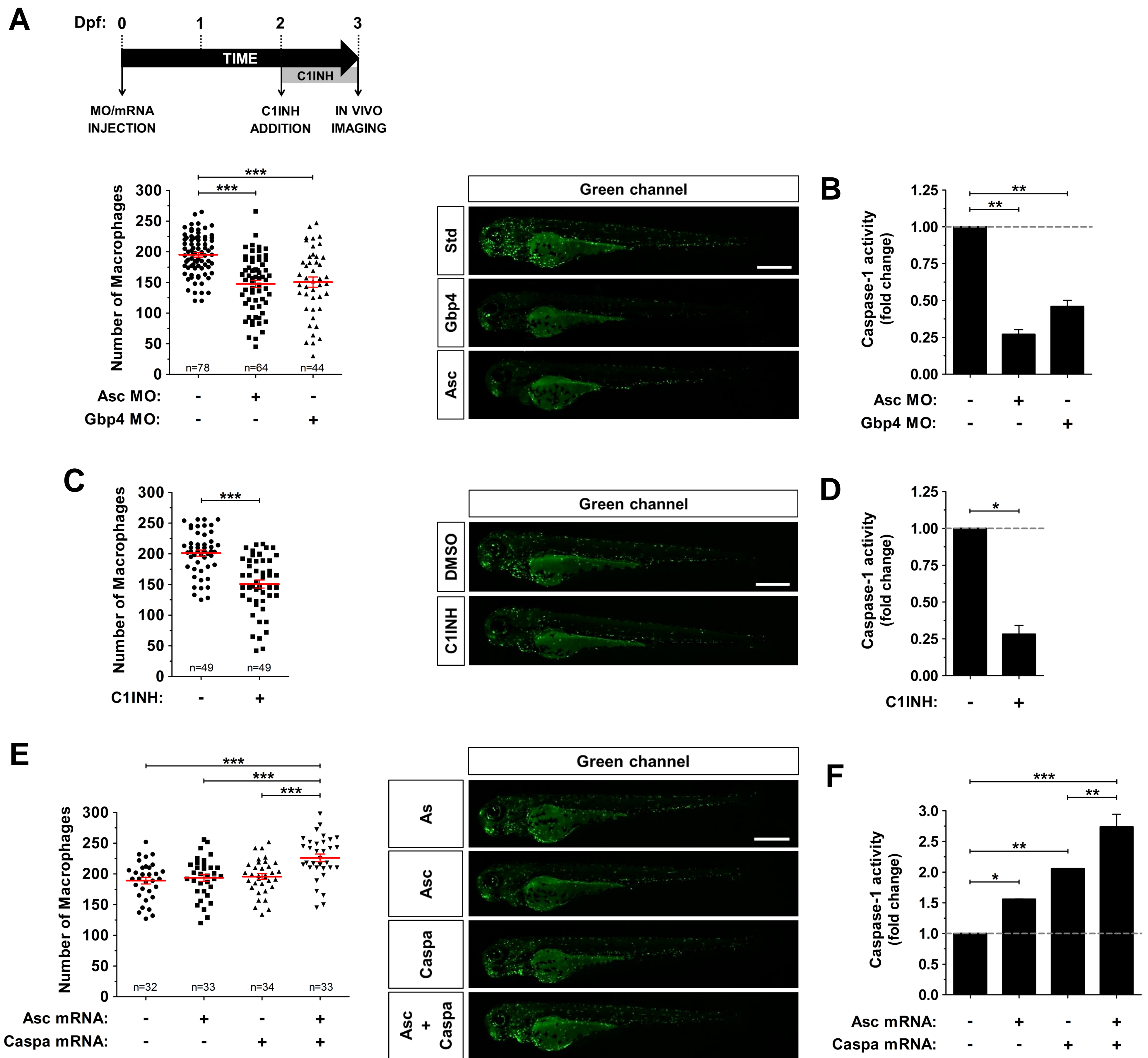


Figure S1. Inflammasome inhibition decreases the number of macrophages in zebrafish larvae. Related to Figure 1. *Tg(mpeg1:eGFP)* zebrafish one-cell embryos were injected with standard control (Std), Asc or Gbp4 MOs (A, B), or with antisense (As), Asc or/and Caspa mRNAs (E-F). Alternatively, *Tg(mpeg1:eGFP)* embryos were dechorionated manually at 48 hpf and treated by immersion with DMSO or the irreversible caspase-1 inhibitor Ac-YVAD-CMK (C1INH) (C, D). Each dot represents the number of macrophages from a single larva, while the mean \pm SEM for each group is also shown (A, C, E). The sample size (n) is indicated for each treatment. Representative images of green channels of whole larvae for the different treatments are also shown. Scale bars, 500 μ m. Caspase-1 activity in whole larvae was determined for each treatment at 72 hpf (one representative caspase-1 activity assay out of the three carried out is shown) (B, D, F). * p <0.05; ** p <0.01; *** p <0.001 according to ANOVA followed by Tukey multiple range test.

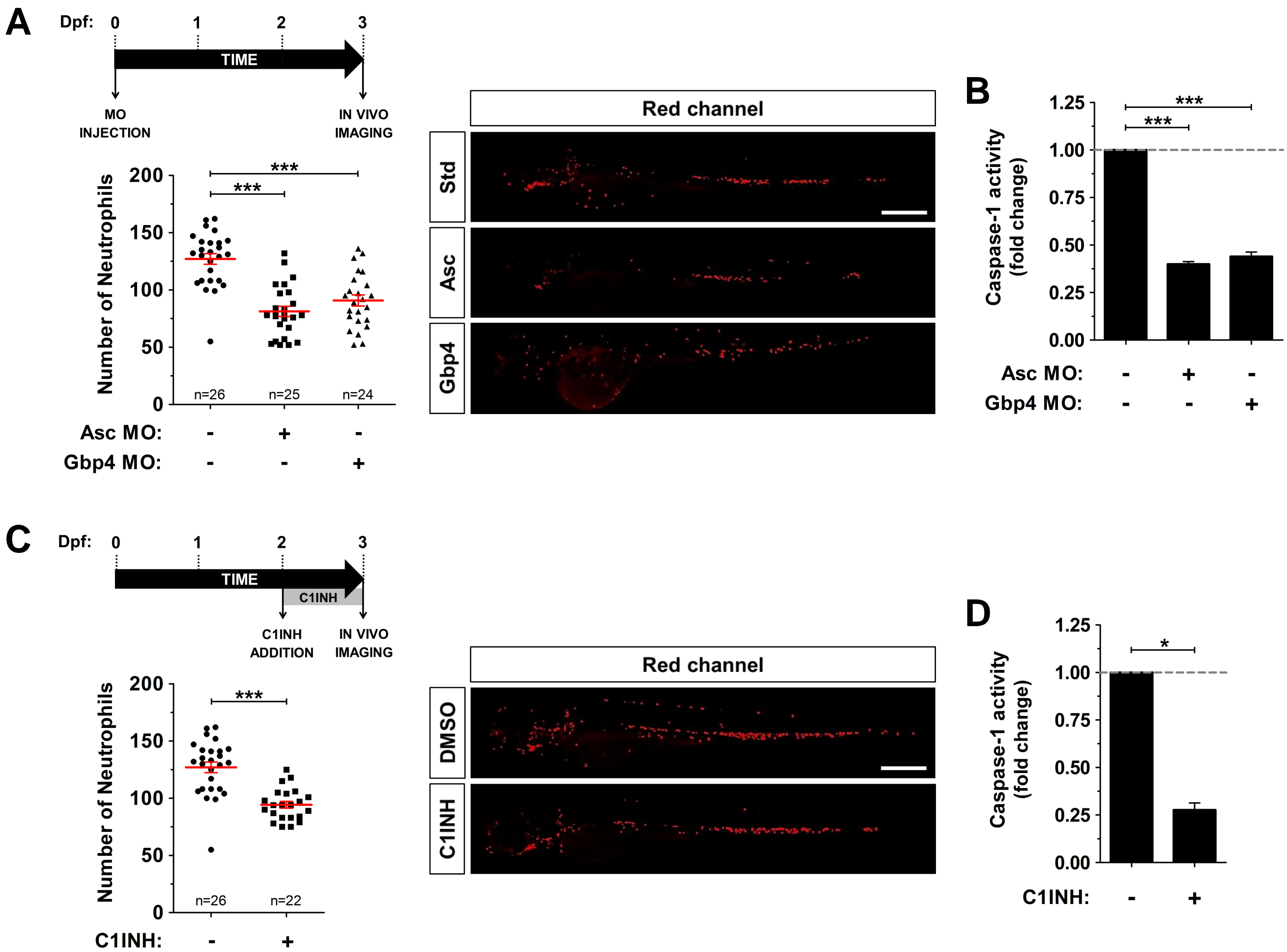


Figure S2. Inflammasome inhibition decreases the number of neutrophils in zebrafish larvae. Related to Figure 1. *Tg(lyz:dsRED)* zebrafish one-cell embryos were injected with standard control (Std), Asc or Gbp4 MOs (A, B). Alternatively, *Tg(lyz:dsRED)* larvae were manually dechorionated at 48 hpf and treated by immersion with DMSO or the irreversible caspase-1 inhibitor Ac-YVAD-CMK (C1INH) (C, D). Each dot represents the number of neutrophils from a single larva, while the mean \pm SEM for each group is also shown. The sample size (n) is indicated for each treatment. Representative images of red channels of whole larvae for the different treatments are also shown (A, B). Scale bars, 500 μ m. Caspase-1 activity was determined in whole larvae for each treatment at 72 hpf (one representative caspase-1 activity assay out of the three carried out is shown). (B, D). * $p < 0.05$; *** $p < 0.001$ according to ANOVA followed by Tukey multiple range test.

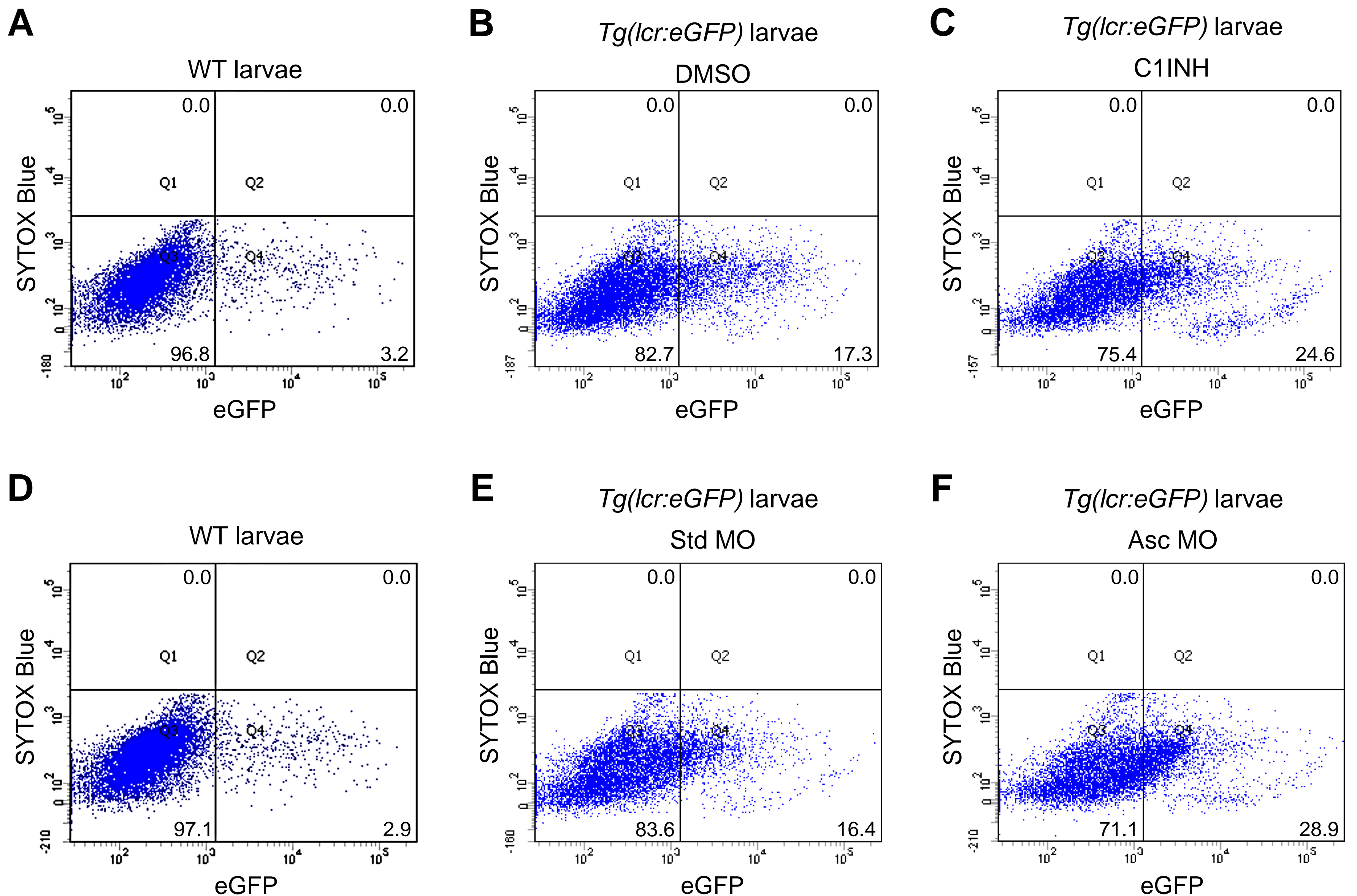


Figure S3. Representative dot plots of green and blue channels of cells from wild type and *Tg(lcr:eGFP)* zebrafish larvae. Related to Figure 1. Wild type (A, D) and *Tg(lcr:eGFP)* (B, C, E, F). zebrafish embryos were manually dechorionated at 24 hpf and treated by immersion with DMSO or the irreversible caspase-1 inhibitor Ac-YVAD-CMK (C1INH) during 48 h (B, C). Alternatively, *Tg(lcr:eGFP)* one-cell embryos were injected with standard control (Std) or Asc MOs (E, F). The percentage of cells in each quadrant is shown.

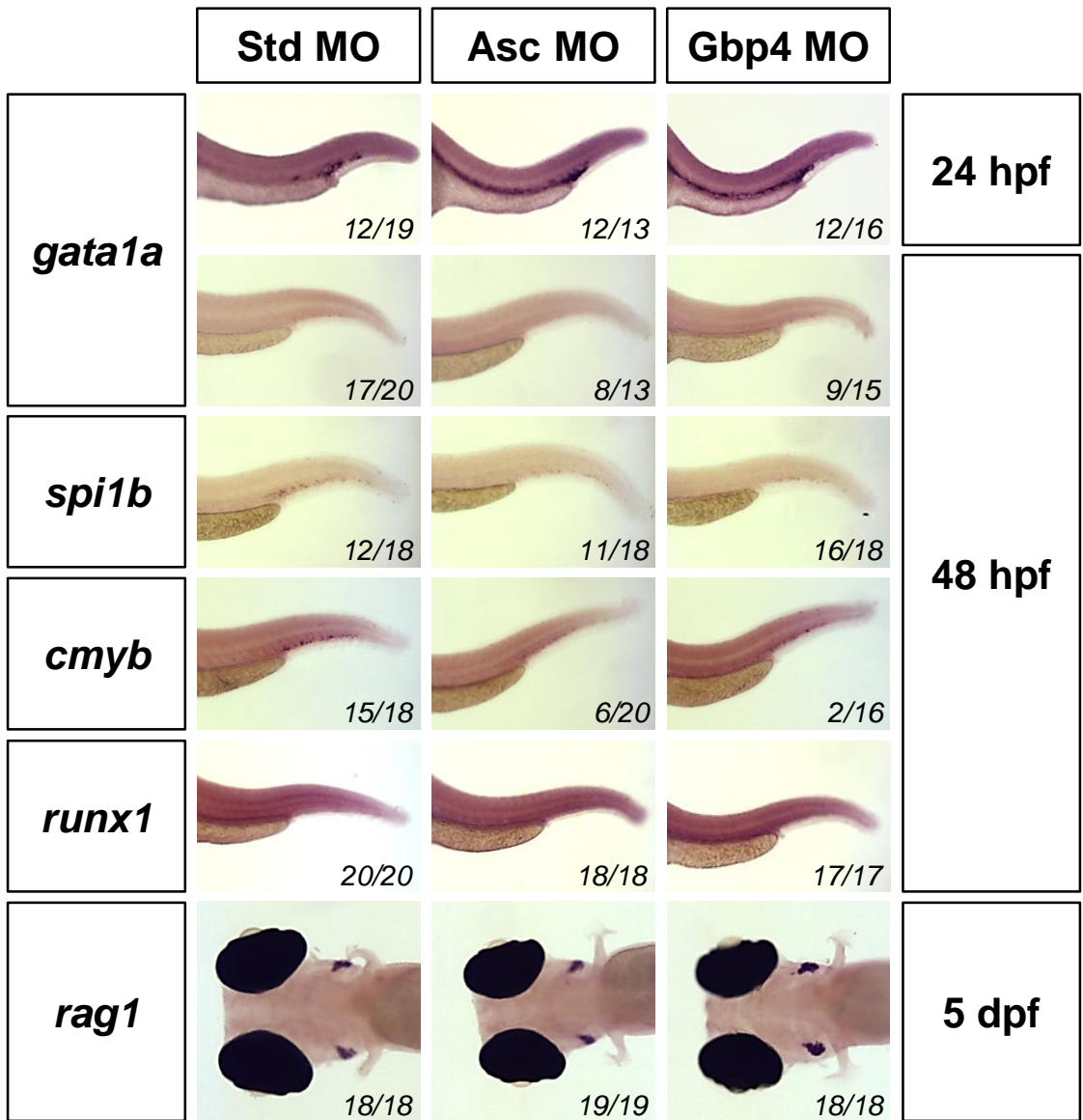


Figure S4. Inflammasome activity regulates *gata1* expression levels in zebrafish larvae. Related to Figures 1 and 2. Casper zebrafish one-cell embryos were injected with standard control (Std), Asc or Gbp4 MOs. At the indicated times, whole-mount *in situ* hybridization (WISH) was performed using antisense probes to the *gata1a*, *spi1b*, *gcsfr*, *cmyb*, *runx1* and *rag1* genes. Numbers in pictures represent the animals with the shown phenotype per total analyzed animals.

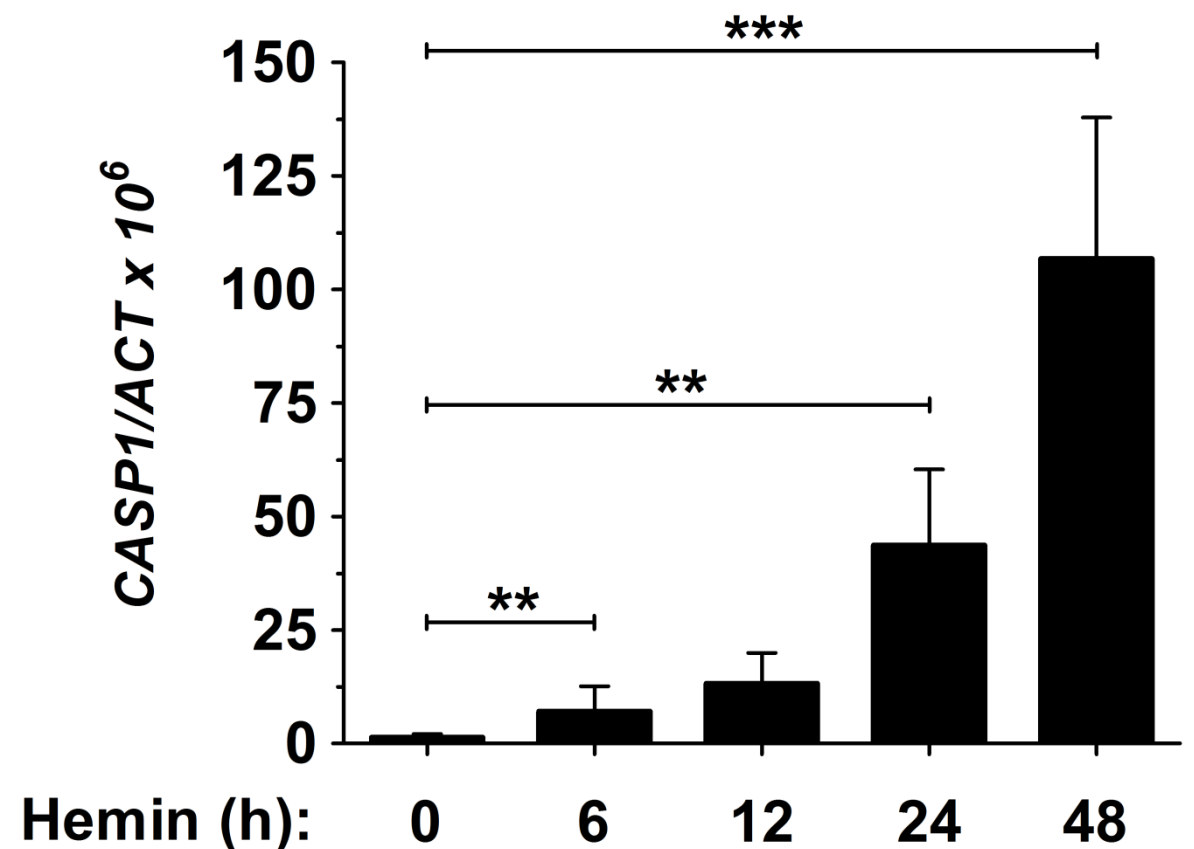
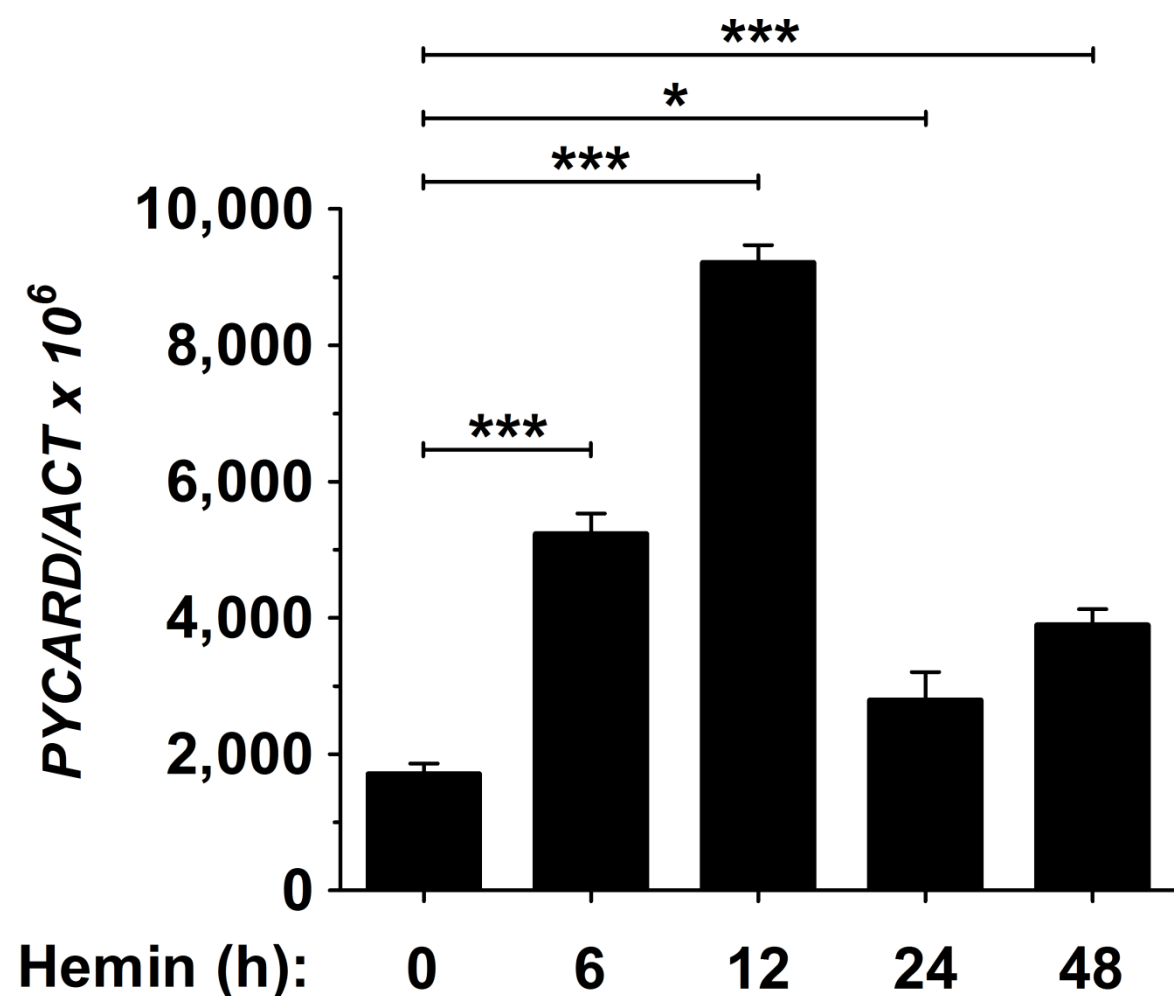
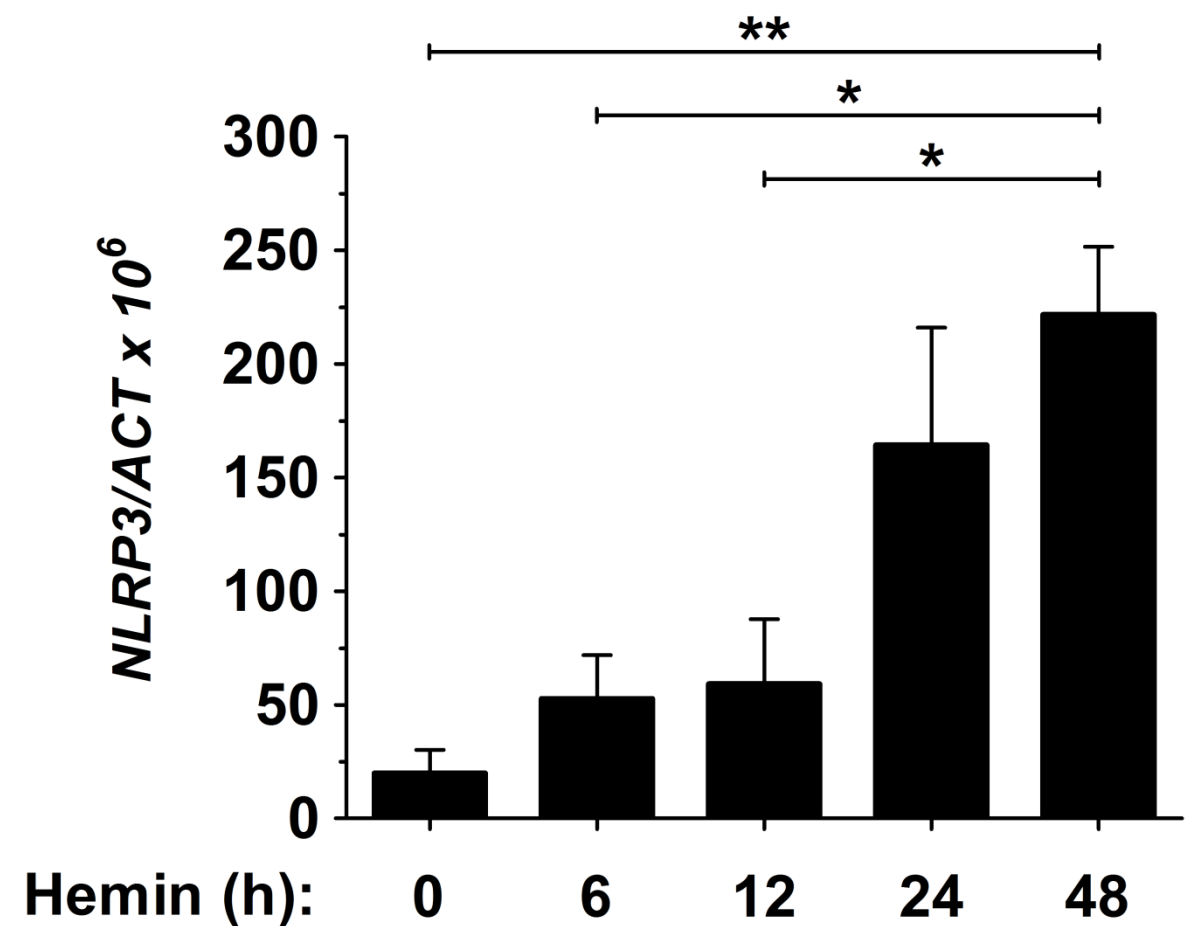
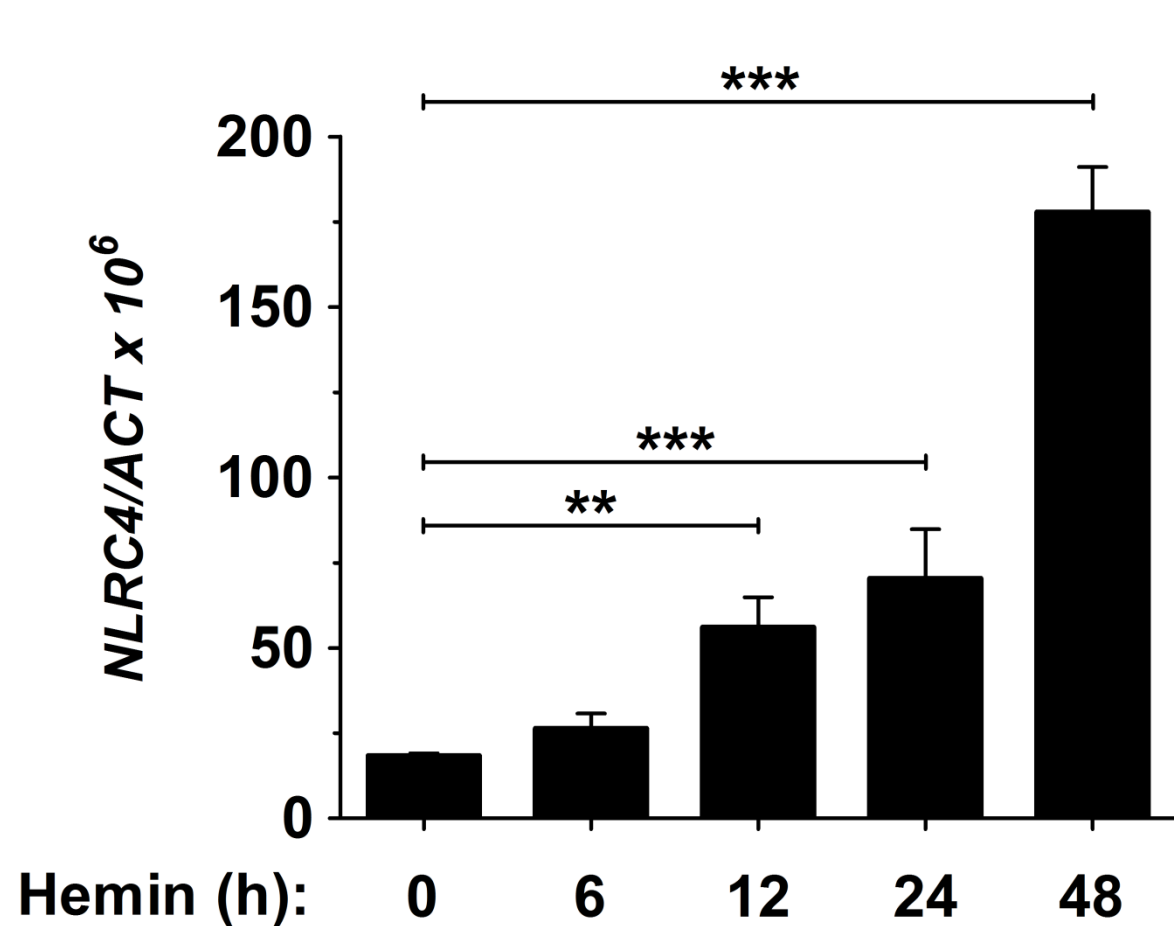


Figure S5. The expression of genes encoding inflammasome components are regulated during the erythroid differentiation of K562 cells. Related to Figure 6. K562 cells were incubated with hemin for 48 h and then the mRNA levels of the genes *NLRC4*, *NLRP3*, *PYCARD* and *CASP1* were determined by RT-qPCR (n=3). The results are shown as the mean \pm SEM. *p<0.05; **p<0.01; ***p<0.001 according to ANOVA followed by Tukey multiple range test.

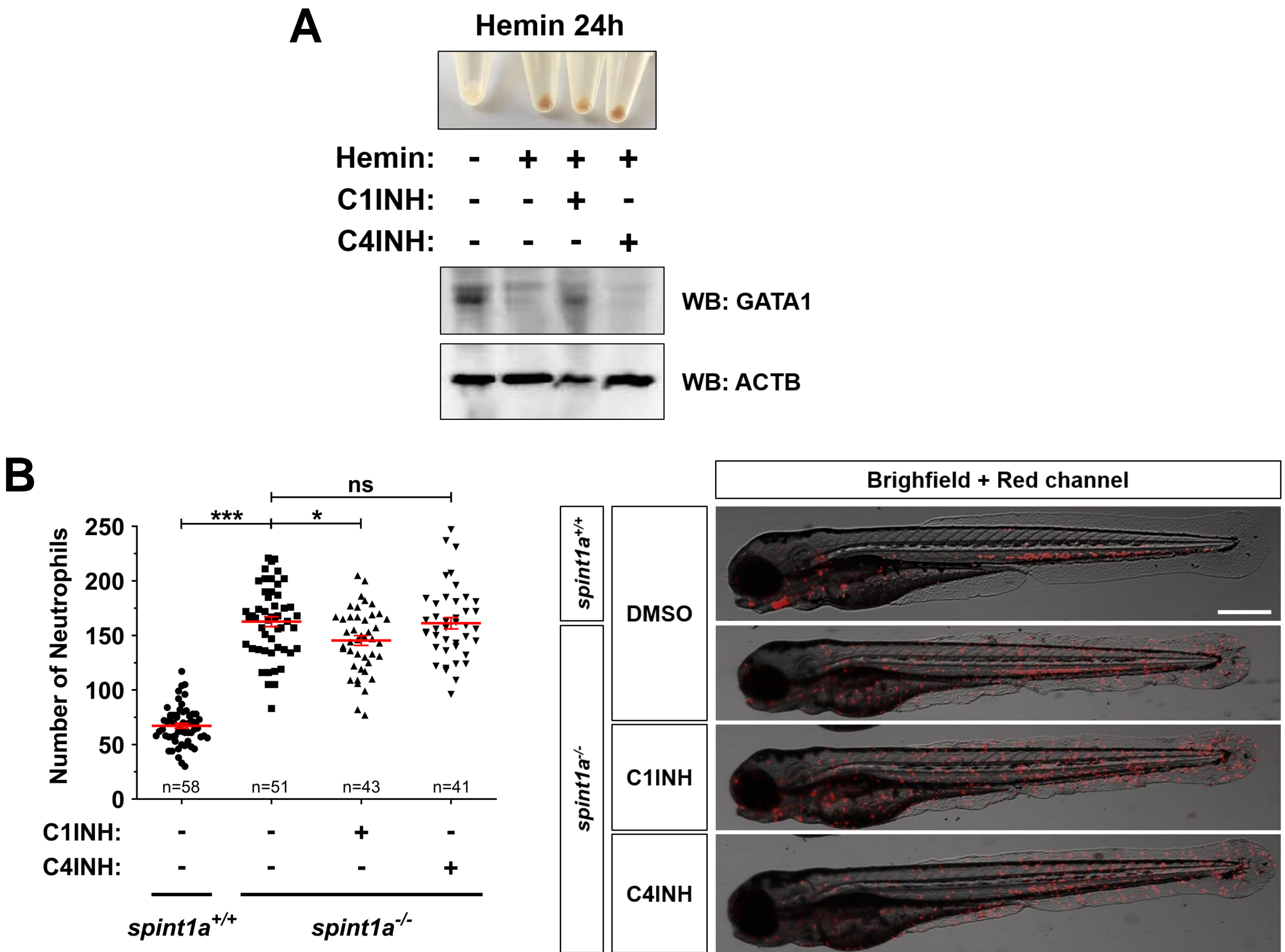
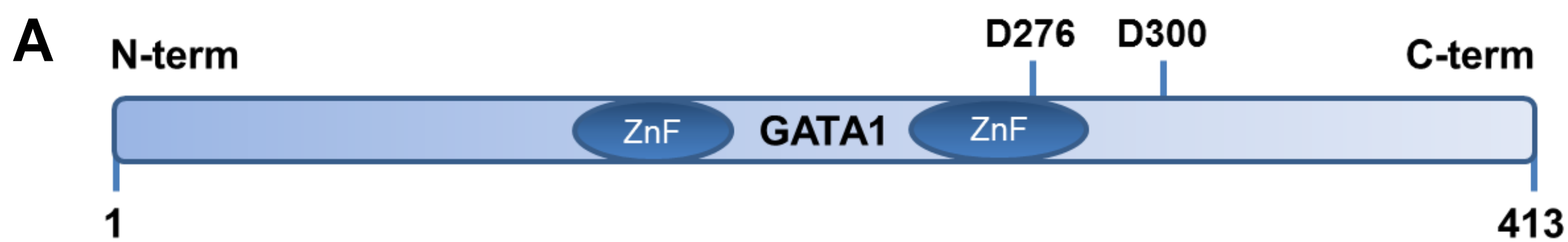
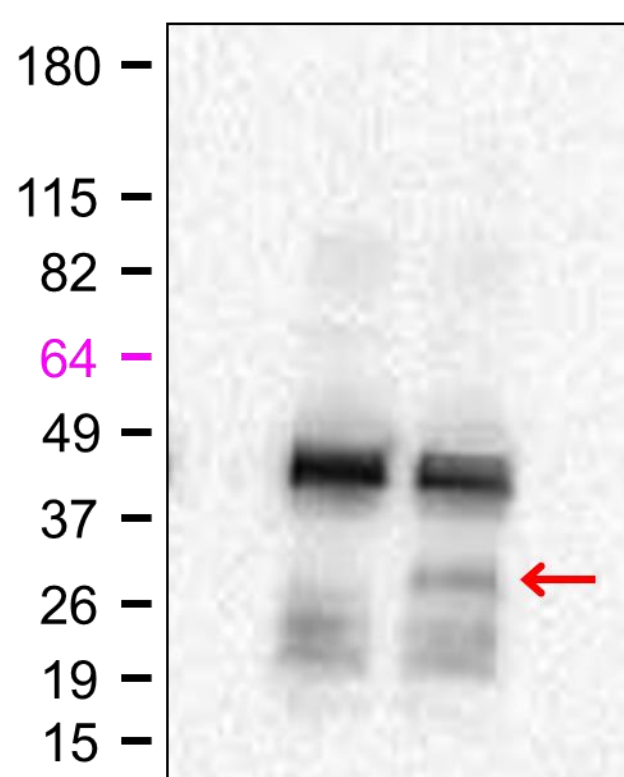


Figure S6. Pharmacological inhibition of caspase-4/caspase-5 failed to regulate erythroid differentiation of K562 cells and neutrophil numbers in zebrafish. Related to Figures 6 and 7. (A) K562 cells were incubated with 50 μ M hemin for 24 h in the presence or absence of the caspase-1 inhibitor Ac-YVAD-CMK (C1INH, 100 μ M) or the caspase-4/caspase-5 inhibitor Ac-LEVD-CHO (C4INH, 100 μ M) and the cell pellets imaged, lysated and resolved by SDS-PAGE and immunoblotted with anti-GATA1 and anti-ACTB antibodies. (B) *spint1a* mutant larvae were manually dechorionated and treated from 1-3 dpf with Ac-YVAD-CMK (C1INH, 100 μ M) or Ac-LEVD-CHO (C4INH, 100 μ M). The number of neutrophils was then determined. Each dot represents the number of neutrophils from a single larva, while the mean \pm SEM for each group is also shown. The sample size (n) is indicated for each treatment. Representative overlay images of green and bright field channels of whole larvae for the different treatments are shown. One representative hemoglobin accumulation (A) and western blot (A) assay out of the three carried out is shown. Scale bar, 500 μ m. ns, not significant; * p <0.05; *** p <0.001 according to ANOVA followed by Tukey multiple range test.



B

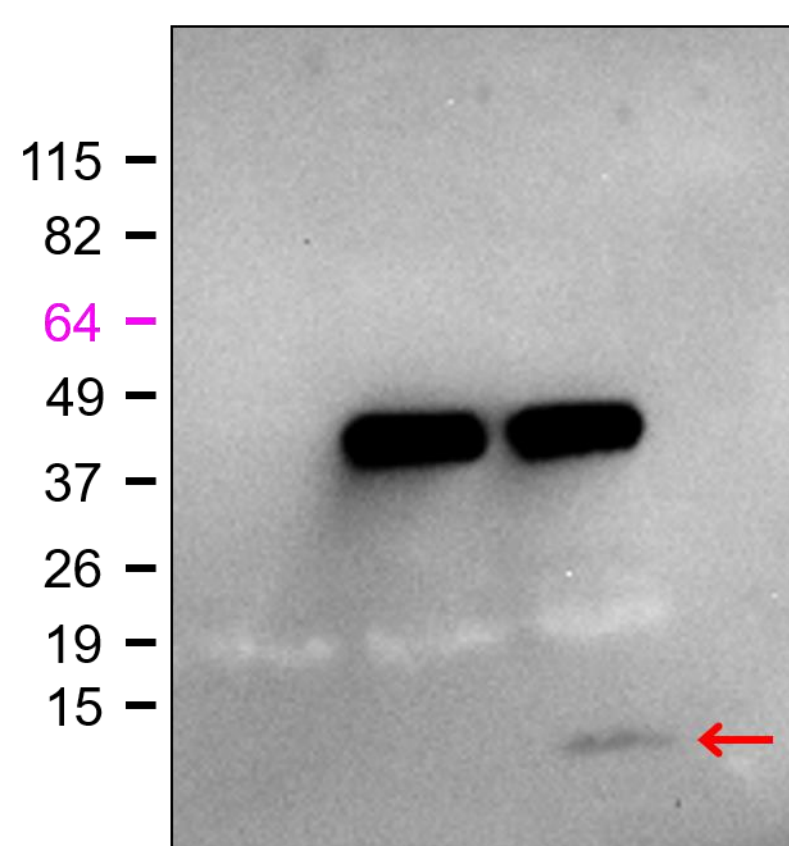
FLAG-PCDNA:	+	-	-
FLAG-GATA1:	-	+	+
rCaspase-1:	+	-	+



IP: FLAG
WB: FLAG

C

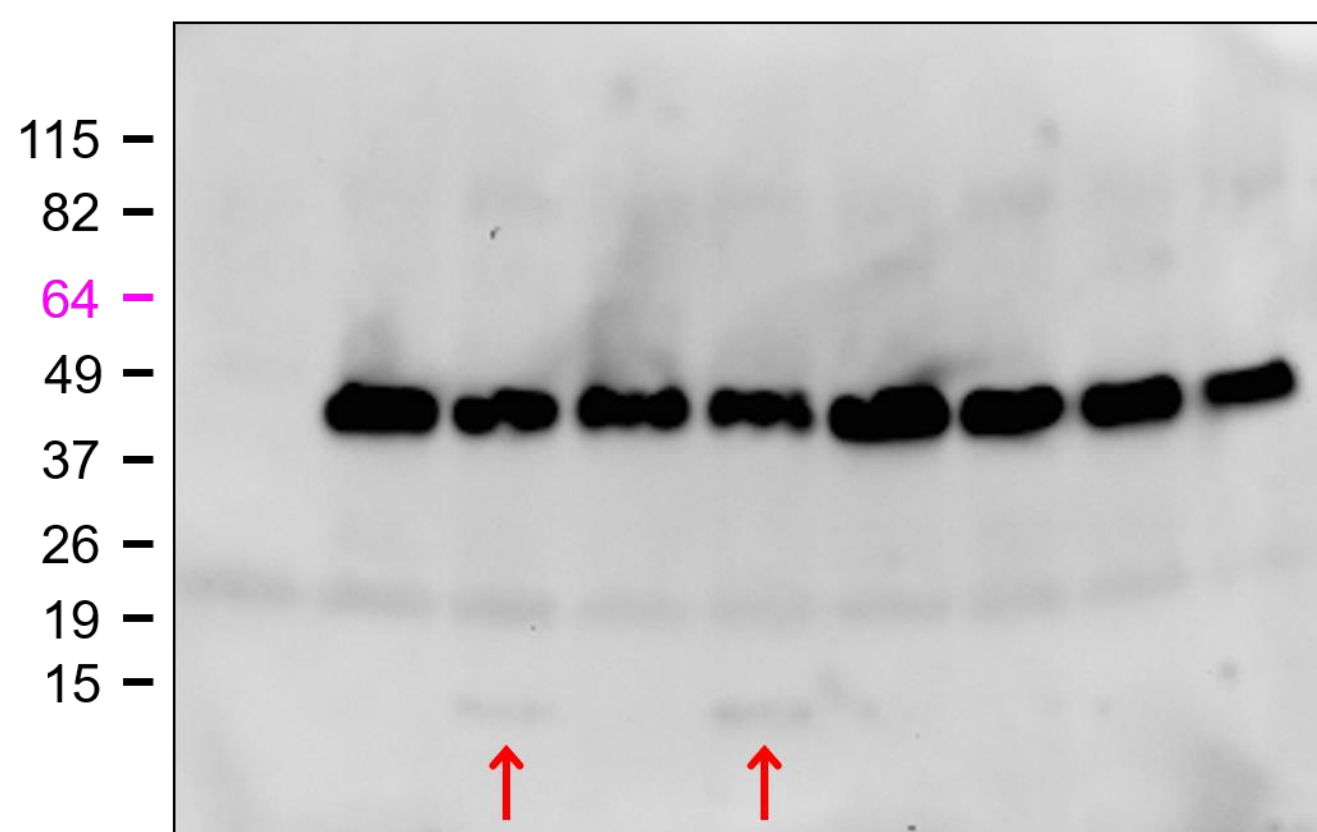
FLAG-PCDNA:	+	-	-
FLAG-GATA1:	-	+	+
rCaspase-1:	+	-	+



IP: FLAG
WB: GATA1 (C-term)

D

PCDNA-FLAG:	+	-	-	-	-	-	-	-	-
GATA1-FLAG WT:	-	+	+	-	-	-	-	-	-
GATA1-FLAG(D276E):	-	-	-	+	+	-	-	-	-
GATA1-FLAG(D300E):	-	-	-	-	-	+	+	-	-
GATA1-FLAG DM:	-	-	-	-	-	-	-	+	+
rCaspase-1:	+	-	+	-	+	-	+	-	+



IP: FLAG
WB: FLAG

Figure S7. Caspase-1 cleaves *in vitro* human GATA1 in residue D300. Related to Figure 6. (A) Scheme of human GATA1 showing the zinc finger domains and residues D276 and D300. (B-D) HEK293T cells were transfected with FLAG-empty or FLAG-GATA1 (B, C) and empty-FLAG, GATA1-FLAG wild type, GATA1-FLAG(D276A), GATA1-FLAG(D300E) or GATA1-FLAG(D276E/D300E) (DM) (D) expression plasmids. Twenty four hours after transfection, GATA1 was pulled down from cell extracts with anti-FLAG M2 affinity gel and treated or not for 2 h at 37°C with 10 IU human recombinant caspase-1. Full length GATA1 and the generated proteolytic fragments were resolved in SDS-PAGE and immunoblotted with anti-FLAG to visualize N-term (B) and C-term (D) GATA1, or anti-GATA1 to visualize C-term GATA1 (C). One representative western blot assay out of the two carried out is shown.

Table S1. Morpholinos used in this study. Related to Figures 1, 2 , 4, 7, S1 and S2.

The gene symbols followed the Zebrafish Nomenclature Guidelines (http://zfin.org/zf_info/nomen.html).

Gene	Ensembl ID	Target	Sequence (5'→3')	Concentration (mM)	Reference
<i>pycard</i>	ENSDARG00000040076	atg/5'UTR	GCTGCTCCTTGAAAGATTCCGCCAT	0.6	Tyrkaska et al., 2016
<i>gfp4</i>	ENSDARG00000068857	e1/i1	GCTGTTTGTGTGTCTCTAACCTGTT	0.1	
<i>gata1a</i>	ENSDARG00000013477	e1/i1	GTTTGGACTCACCTGGACTGTGTCT	0.2	Galloway et al., 2005

Table S2. Primers used in this study for RT-qPCR. Related to Figure 4 and S5. The gene symbols followed the Zebrafish Nomenclature Guidelines (http://zfin.org/zf_info/nomen.html). ENA, European Nucleotide Archive (<http://www.ebi.ac.uk/ena/>).

Gene	ENA ID	Name	Sequence (5'→3')/Vendor
<i>rps11</i>	NM_213377	F1	GGCGTCAACGTGTCAGAGTA
		R1	GCCTCTTCTCAAAACGGTTG
<i>gata1a</i>	NM_131234	F1	CGTTGGGTGTCCCCCGGTCT
		R1	ACGAGGCTCGGCTCTGGACG
<i>spi1b</i>	NM_198062	F1	TGTTACCCTCACAACGTCCA
		R1	GCAGAAGGTCAAGCAGGAAC
<i>gcsfa</i>	FM174388	F1	TGAAGCAACGACCCTGTCGCA
		R1	CCGCGGCCTCAGTCTGGAAA
<i>mcsfa</i>	NM_001114480	F1	AGCCCACAAAGCCAAGGTAA
		R1	CTGACGCTCTGTGAAGGTGT
<i>ACTB</i>	NM_001101	H_ACTB_1	Sigma-Aldrich
<i>PYCARD</i>	NM_013258	H_PYCARD_1	
<i>CASP1</i>	NM_001257118	H_CASP1_1	
<i>NLRC4</i>	NM_001199138	H_NLRC4_1	
<i>NLRP3</i>	NM_001243133	H_NLRP3_1	